DETAILED RESISTIVITY AND SEISMIC REFRACTION SURVEY OF MASARI/KAFUR KIMBERLITE PIPE AREA, NEAR MALUMFASHI, KADUNA STATE.

BY

ABRAHAM ONUGBA

Thesis, submitted to the Ahmadu Bello University, in partial fulfilment of the requirements for the award of the degree of

MASTER OF SCIENCE IN APPLIED GEOPHYSICS

DEPARTMENT OF PHYSICS
AHMADU BELLO UNIVERSITY
ZARIA - NIGERIA.

JULY, 1979

A C K N O W L E D G E M E N T

I am most grateful and thankful to God through Jesus Christ for His grace and mercy by which I have been able to carry out this work.

Special gratitude is due to Professor O. E. Ajakaiye, the Head of Physics Department (Ahmadu Bello University, Zaria) who supervised this work. Her advices and encouragement throughout my course of study, her useful suggestions on the field work and her comments on the draft of this thesis are highly appreciated.

I wish to thank other members of staff in the Physics Department who in one way or the other contributed to the success of this work. I sincerely thank Mr. S. E. Ananaba for his useful suggestions and guidance during the writing of the manuscript and also for his kindness in providing necessary references; I am grateful to: Mr. P. J. T. Verheijen who suggested the survey area; Messrs S. B. Osazua, M. Daniyan, Dr. M. W. Asten and Dr. E. E. Myada for their useful suggestions and criticism during the field work. The use of a resistivity modelling computer programme belonging to Mr. Verheijen and

Dr. Aston is sincerely acknowledged. I appreciate the kindness of Paterson et al (1977) who sent me a copy of their report and Mr. Abba of Geology Department (A.B.U.) who read and adviced the geology aspect of this work.

I also appreciate the kindness of Messrs Haruna (Hospital Secretary), Stephen Omeje, SN Daniel A. Okoliko and Daniel Ejeh all of A.B.U. Teaching Hospital, Malumfashi.

I am deeply indebted to Mr. Abdullayi S. Ocheni of Department of Chemistry, (A.B.U., Zaria) who typed the thesis.

I give thanks and praises to God for Mrs. Rehab I. Onugbo, my wife, whose good understanding, patient endurance and words of encouragement comforted me throughout my course of study; I cannot forget Abel S. Agbaji and other Christian brethren who prayed for me and encouraged me.

I am sincerely grateful to the Ahmadu Bello University, Zaria, who sponsored the whole course of study and the Advanced Teachers' College, Katsina-Ala, that granted me study leave.

Finally, I tender sincere apology for any over sight.

CONTENTS

	Page
Acknowledgement	i
List of Figures	vi
List of tables	viii
Abstracts	x
CHAPTER I	
Introduction	1
CHAPTER II	
Geology	3
2.1 Geology of Kimberlites	3
2.2 General Geology of the Kafur/Masari area	6
2.3 The Kafur/Masari Kimberlite pipe ..	8
CHAPTER III	
Previous Work in the Area	11
3.1 Geological Investigations	11

Page

CHAPTER IV

The present Survey, Choice of Method and Field Techniques 16

4.1 Introduction 16

4.2 Choice of Methods 17

4.2.1 Resistivity Methods 19

4.2.2 Seismic Refraction Method 26

4.3 Field Techniques 29

CHAPTER V

Interpretation 32

5.1.1 Resistivity Profiles 32

5.1.2 Vertical Electrical Soundings 39

5.2 Interpretation of Seismic Refraction Data 53

CHAPTER VI

Discussion 66

6.1 The Results 66

6.1a Resistivity Profiling 66

6.1b Correlation between Refraction Results, Resistivity Anomaly and Local Geology .. 68

6.1c Existance of Kimberlite and Groundwater .. 69

		Page
6.1d	Structural Trend-line and Kimberlite Emplacement	71
6.2	Conclusion	73
6.3	Recommendations	74
REFERENCES	.. ..	76

LISTS OF FIGURES

Figure No.	Title	Following Page
1	Location of Survey Area	2
2.1	A typical weathered kimberlite ..	4
2.2	The Geological Location of the Kafur/ Masari Kimberlite pipe	6
3.1	Contour map of Bougner anomaly ..	12
3.2	Observed and Calculated gravity anomaly along profile CD and its causative body ..	13
3.3	Contour map of vertical magnetic field in the area	13
3.4	Observed and Calculated magnetic anomaly along profile AB	13
3.5	Apparent resistivity profiling over the pipe	15
4.1	The electrode arrangement used for electrical resistivity measurements	23
4.2	Field set-up of TRIO system ..	28
4.3	Geophysical survey map (showing outline of pipe at 20 m depth	31
5.1	Apparent resistivity with elevation, on traverse Yo and 5	35
5.2- 5.7	Apparent resistivity profilings on traverses X_0, X_1, ta..X_5	37

Figure No.	Title	Following Page
5.8 - 5.9	Apparent resistivity contour for 5 m and 20 m electrode spacings respectively	38
5.10 - 5.17	VES A to VES H	49
5.18	The geoelectric sections and the corresponding geological interpretations for a kimberlite pipe	51
5.19	Ray paths of critically refracted rays used in determining time-depth to refractor	53
5.20	Travel-time curves with seismic sections for measurements on Traverse Yo Spread 2 and 3	58
5.21	Travel-time curves and the corresponding seismic sections for refraction measurements on traverse Yo - the baseline ..	60
5.22	Travel-time curves and the corresponding seismic sections for refraction measurements on traverse X_1	62
5.23	Travel-time curves and seismic sections for traverse X_5	63

LISTS OF TABLES

Table	Title	Page
3.1	Combined seismic and resistivity interpretation (after Verheijen and Ajakaiye, 1979)	15
5.1	Resistivity ranges for some sediments rocks and minerals (Telford et al, 1976)	43
5.2	Summary of the results of VES measurements at each sounding point	52
5.3	Representative velocity values (Mooney, 1977)	57

A B B R E V I A T I O N S

NE	North-East
SW	South-West
SE	South-East
NW	North-West
m	metre
msec	millisecond
g.u.	gravity unit
V.E.S.	Vertical electrical sounding
m/sec	meter per second

A B S T R A C T

Near Masari/Kafur in Kaduna state an intrusion suspected to be a kimberlite pipe has been investigated using some geophysical survey methods. The electrical resistivity profiling technique delineated the pipe in details, while electrical resistivity soundings and seismic refraction measurements established the surficial layer structure of the pipe. From these measurements it was deduced that the Masari/Kafur kimberlite pipe is between 560 and 660 m long with a maximum width of 140 m and is oriented in a direction east of NE. The surface of the pipe is covered by 6.B m of soil and gravel with seismic velocity ranging from 500 to 870 m/s and mean resistivity of 210 ohm-m. The second layer has a seismic velocity of 2000 to 2.60 m/s, a mean apparent resistivity of about 13 o h m - m and a thickness range af 17 to *34* m. The existence of a third layer was detected. It has n seismic velocity between 3260 and 3450 m/s and average apparent resistivity of over 1000 ohm-m.

Correlation of these results with previously measured gravity and magnetic anomalies over the same pipe as well, as

with geophysical anomalies reported over known kimberlite pipes in other parts of the world confirm that the Kafur/ Masari is indeed a kimberlite pipe.

C H A P T E R I

INTRODUCTION

Kimberlite pipes are important and much searched for because of their close association with diamonds and other inclusions. Diamon is a most desired gemstone the world over, for personal adornment and decorative purpose as well as for its unique physical properties; it is the hardest substance known, has a single element (carbon), and is durable with a high refractive index and disperson (Gntaman 1967). Kimberlites contain inclusions of ultrabasic types believed to have originated in the upper mantle. These inclusions are helpful to geochemists and petrologists who investigate the nature of the upper mantle and the origin of basalts.

In Nigeria an intrusive rock believed to be kimberlite pipe has been located in Kafur - Maseri area, Kaduna State. It is situated in an almost level plain at latitude $7^{0}41.9$ N and longitude $11^{0}37.6$ E, SE of Maseri and over 1 km SSE of Kafur (fig. 1).

An earlier reconnaissance geophysical work has been carried out over this suspected kimberlite pipe (Verhoyen and Ajakaiye, 1979). The present work is a follow-up of the earlier work with more detailed geophysical surveying to ascertain the exact location, extent and possible physical properties of the suspected intrusion and to find out whether there are more than one pipes in the area. Thus detailed direct-current resistivity and seismic refraction measurements were carried out over the extent of the pipe.

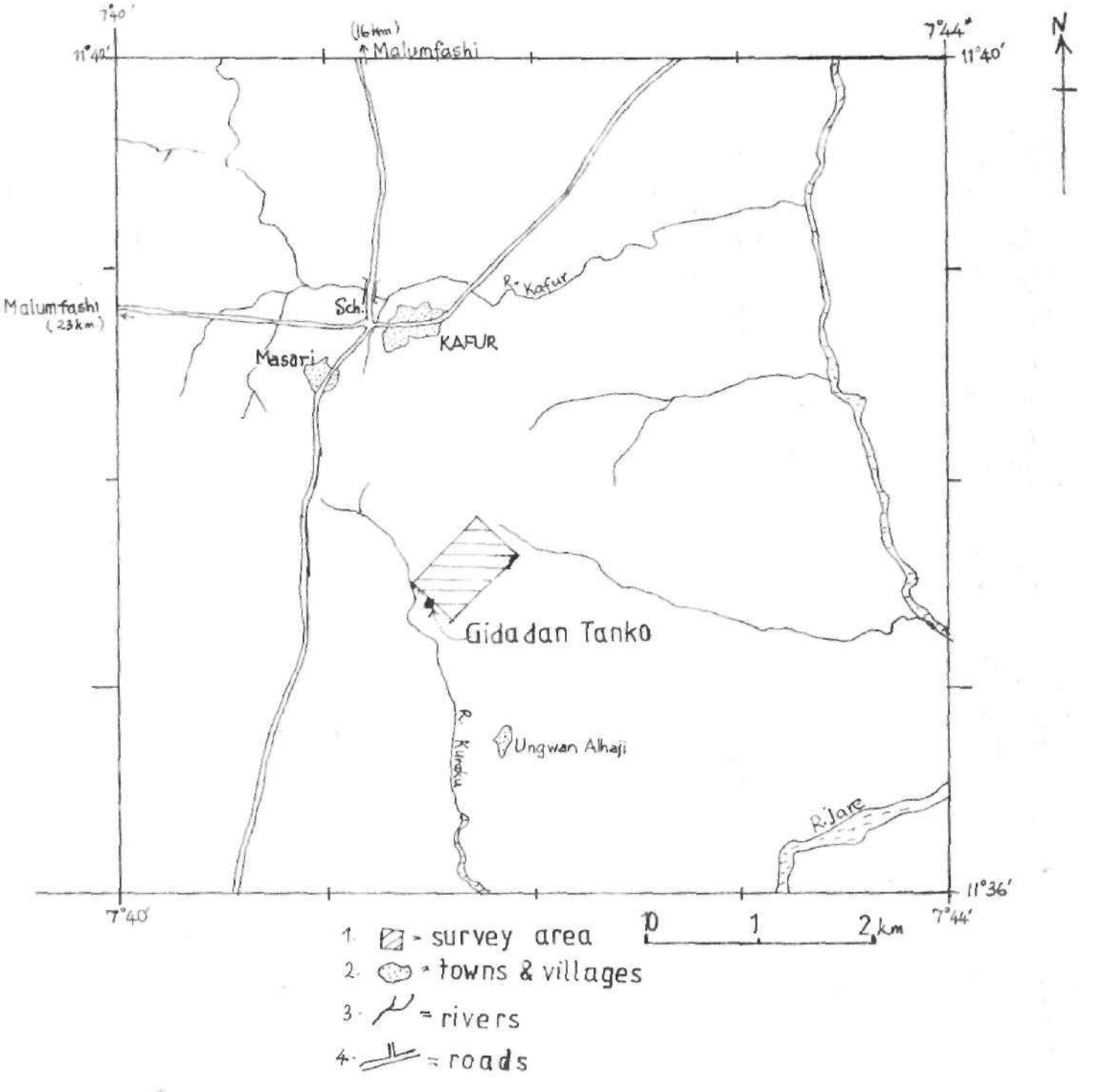


FIG.1 LOCATION OF SURVEY AREA

C H A P T E R II

GEOLOGY

2.1 GEOLOGY OF KIMBERLITES

Kimberlites are intrusive ultramafic rocks. They have been found to consist mainly of olivine and pyroxine, the common constituents being ilmenite, garnet, magnetite chrome diopside and most importantly (but not essentially) diamonds (Bateman 1967; Dawson, 1967 and Paterson et al 1977). Paterson et al further noted that over 10% of known kimberlites contain considerable amounts of diamonds.

Kimberlites occur as small pipes or diatremes and dykes. The dykes which are generally narrow, rarely more 10 m in width, may be tens of kilometer long. They often occur in swarms which appear in parallel. The pipes occur in groups of two or three, and in rare cases, up to 70 pipes are located close to dykes to which they are often connected. Known pipes have been found to lack unique shape and the size (or the surface extent) may vary between less than 50 m to over 1 km.

Pipes are known to decrease in size with depth. They are usually vertical (Bateman 1967).

It has been found that kimberlites are located in the interior and margins of stable continental areas as well as in orogenic belts although those intrusions in the younger orogens are largely barren (Clifford, 1972).

Three broad kinds of rock types may be encountered in a kimberlite body. They are, in the following sequence, (1) the 'yellow ground' at the surface, (2) "blue ground" and (3) the "hardebank" Dawson, 1967 and Paterson et al, 1977. The yellow ground is the decomposed or oxidized kimberlite. Paterson has said that in a typical kimberlite (fig. 2.1) the yellow ground consiting meinly of clay materials montronite and montmorillonite, may be found up to a depth from 10 m to hundreds of meters. The blue ground which lies below the yellow ground is the same rock in a better state of preservation. The hardebank is the hard unweathered kimberlite. Actually the distribution of these rock types is believed to be controlled by the depth of surface weathering and percolating ground water. Kimberlite body has a fixed amount of water which on the average has been found to be 7.7%. Many inclusions of overlying and underlying rocks are contained in kimberlites.

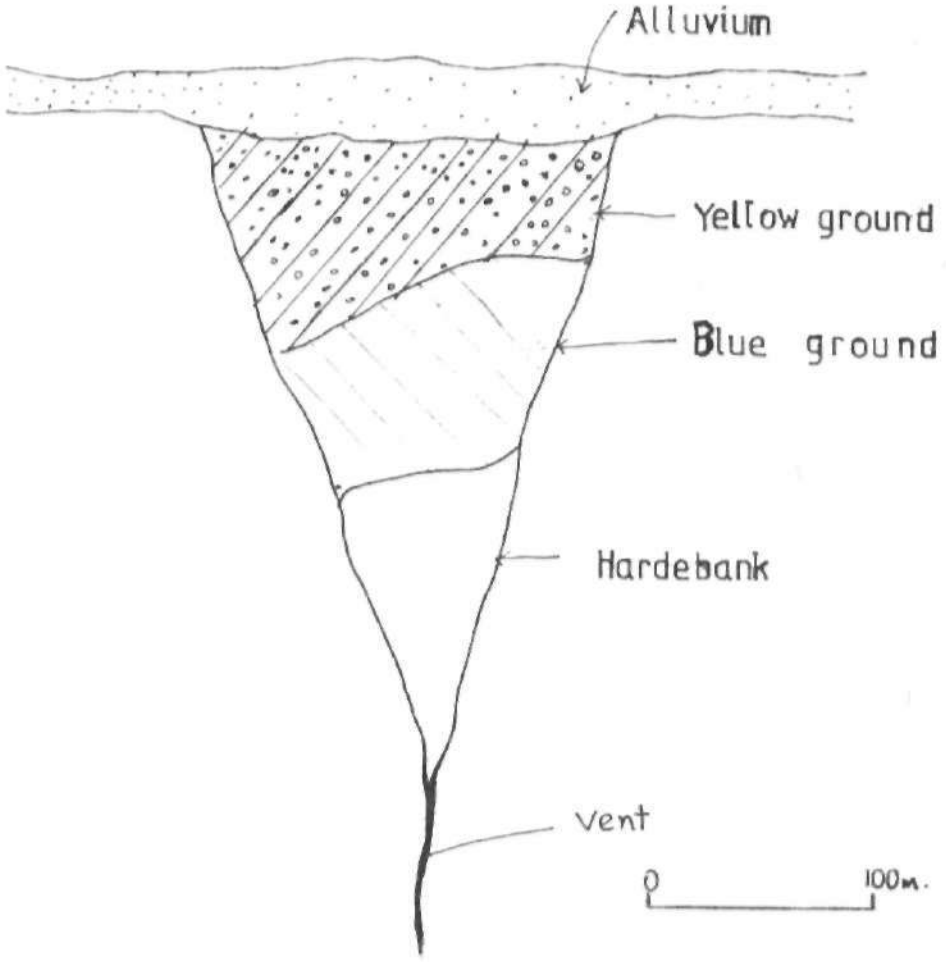


FIG. 2.1 A Typical Weathered Kimberlite (after Paterson et al 1977)

The inclusions from underlying rocks, particularly the ultrabasic rock-types, are believed to have originated from the upper mantle. Geochemists and experimental petrologists attach much importance to these, in connection with investigations on the nature of the upper mantle and the origin of basalts.

Unweathered kimberlites have been classified by Dawson (1967) into three types: massive kimberlite, intrusive kimberlite breccia, and kimberlite tuffs and tuff-breccias. The classification is based on the nature of rock fragments contained in each of them which in turn depend on the different mode of emplacement. Dawson has noted that massive kimberlite contains little or no inclusions of country-rock xenoliths. It occurs in dykes, veins or segments of diatremes and is subvolcanic. Intrusive kimberlite breccias contain 20-60% fragments of various rock-types including xenoliths of country-rock fragments amounting to less than 5% of the bulk in kimberlite tuffs while the country-rock is variable in tuff-breccia. This class of kimberlites is found in diatremes or segments of diatremes. The shape of a kimberlite pipe is determined by pre-existing joint pattern or near-surface unconformities while the location of swarms of dyke and groups of pipe

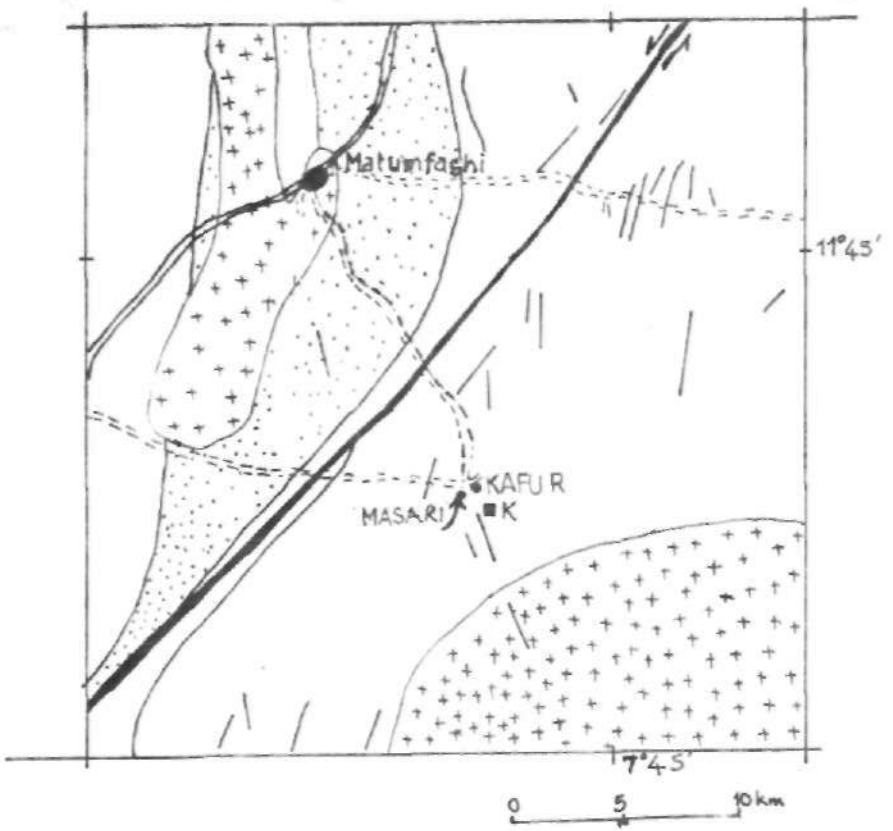
is controlled by location of deep seated tension fractures. (Dawson, 1967).

2.2 GENERAL GEOLOGY OF THE KAFUR/MASARI AREA

Kafur and Masari are two villages about 1 km. apart. They are included in the region (1200 km^2 approximately) around Zaria which was mapped by McCurry between 1968 and 1970. Both villages were found to lie within the basement complex of Northern Nigeria.

The basement complex include rocks older than the late proterozoic metasediments. Oyawoye (1964) grouped the rocks into (1) the ancient (or older) metasediments, (2) the gneisses, migmatites and older granites and (3) the newer (or younger) metasediments. McCurry (1970) described the older metasediments as the remains of an older supracrustal cover, probably of Birrinian age, to distinguish them from the younger metasediments which are the late proterozoic supra crustal sediments.

The area under investigation is located in the basement gneisses (fig. 2.2).



KEY

older granite

proterozoic metasediments

basement gneisses

K kimberlite pipe

roads

transcurrent fault

stuctural trend-line taken from air photograph

N

FIG. 2.2 THE GEOLOGICAL LOCATION OF THE KAFUR KIMBERLITE PIPE (after McCurry 1970)

It is believed that large areas of the basement complex have been converted to migmatite and granite gneiss by intensive processes of metamorphism and granitization which affected the sedimentary sequence. The younger metasediments were assumed deposited on the granitized basement and both were subjected to two phases of synclinal folding during the Pan-African orogeny (McCurry, 1973). The deformational events were accompanied by polyphase metamorphism as well as migmatisation and granitisation of the basement gneiss, resulting in intrusion of a suite of syn- to late-tectonic granites. McCurry reported that jointing, fracturing and faulting following the orogeny could be located in the area she mapped.

One of the faults, a major NE - SW transcurrent fault has been located, close to Nafur-Masari area, at about 7 km. NW of the suspected kimberlite pipe. The fault was found to have displaced the NS trending metasedimentary belt by 10 km., causing a swing in the structural trends in the metasediments by a drag on either of the fault (fig. 2.2). Since near-surface weaknesses such as fracture zones or joints are believed to control distribution of kimberlite pipes the location of these faults, joints and fractures are important in kimberlite explorations.

2.3 THE KAFUR/MASARI KIMBERLITE PIPE

The suspected Kafur/Masari kimberlite pipe is an intrusive body void of surface exposure of its presence in the area. It is situated in an almost level farmland, SE of Masari and about 1 km. SSE of Kafur village, at latitude $7^{0}41.9$ N and longitude $11^{0}37.6$ E. Scattered basement rocks outcrop around the intrusion.

Wright (1976) reported that the pipe intrudes a medium-grained slightly foliated pink-grey basement granite gneiss. This is consistent with McCurry's finding that the country rock is granite-gneiss which locally includes more massive granite observed in nearby rock outcrops (McCurry, 1970; 1973).

The pipe is believed to be a breccia containing fragments of granite gneiss and small rounded pieces of altered basalt Turner (19[illegible]). According to Wright, the Northern section of the pipe contains abundant ilmenite with accessory zircon, olivine, chrome diopside and pyropic garnet; small parts of the Northern section and also the Southern end consist of what he described as fine-grained grey-black kimberlite with ilmenite.

Turner found the rock to be thoroughly decomposed. A typical geologic sequence that he found over the pipe

was silt (1 m), pisolitic laterite with ilmenite crystals (1 m), Clay (2 m) and finally breccia. It is worth noting however that Turner's findings were based on two pits dug which penetrated the intrusion at depths of 2-3 m below the pits are not known.

The Sierra Leone Diamond Company is said to have first located the pipe in 1961. McCurry reported that the company dug pits and trenches in the suspected kimberlite pipe area in 1965 but the results of their findings were not published. The only open pit found in the area during the present survey was observed to be partly infilled to a depth of 1.5 m. But geophysical work carried out in the area (Verheijen and Ajakaiye, 1976) indicate that the rock is deeply weathered.

There have been speculations as regards the age of the pipe. Wright suggested that the pipe intruded the basement rocks during Jurassic time, about 150 m.y. ago. He based his suggestion on the closeness of the pipe to Runko basalt (which is believed to be of Jurassic age) in North Western Nigeria. It has also been correlated with cenozoic volcanics in Nigeria on the basis of petrographic affinities (Turner, 1975).

On the economic aspectsthere is evidence of substantial amount of ilmenite at the site of the pipe. And it is hoped

this pipe may be a source of diamonds. Also much value may be contained in the weathered part of the pipe.

C H A P T E R III

PREVIOUS WORK IN THE AREA

3.1 GEOLOGICAL INVESTIGATION

As stated in Chapter II, the Diamond Corporation of Sierra Leone used heavy mineral sampling method (panning of rivers and soil sampling) to locate the suspected kimberlite pipe, between 1961 and 1965 (McCurry, 1970; Wright, 1976). The report of the work has not been published. However, Wright (1976) reporting on information he obtained from an Anglo American Corporation of South Africa Limited has described the pipe to be about 600 m long, between 30 m and 170 m wide and oriented slightly east of North-east. Two small dykes were found extending from the main pipe but the total extent of these dykes from the pipe were not indicated.

Since the company left in 1965, several geologists and mineral prospectors (McCurry 1970; Verheijen and Ajakaiye 1973; 1975; Turner or Ajakaiye 1975) have visited the site and sunk some pits. Some of the results of their findings have been discussed already in section 2.2. As was pointed

out in the same section the only open pit found at the site during this survey was infilled up to about 1.5 m depth. McCurry (1970) included this site in her geological survey map of Zaria area. Part of the map reproduced in fig. 2.2, show structural trend lines and fault zone close to the suspected kimberlite intrusion. She also analysed several grains of ilmenite (which she reported collected from around pits and) believed to be derived from the suspected kimberlite. The MgO contents of these samples were as much as 4% but with average value around 3%, as against 5 - 12% reported by Dawson (1968) for a typical kimberlite.

3.2 GEOPHYSICAL INVESTIGATIONS

The first published geophysical survey in the area was carried out in 1976 (Verheijen and Ajakaiye, 1976) to detect any anomalies associated with the suspected kimberlite pipe. Gravity and vertical magnetic field survey was carried out over an area of 0.6 $km.^2$

For the gravity measurements a Worden (W135) gravimeter with an instrument constant of 0.8823 $\pm$ 0.0005 g.u/division was used. Their Bouguer anomaly map reproduced (fig. 3.1) indicate an anomaly, elongated in the NE - SW direction. They expected a maximum total error of 0.5 c.u. in their observations.

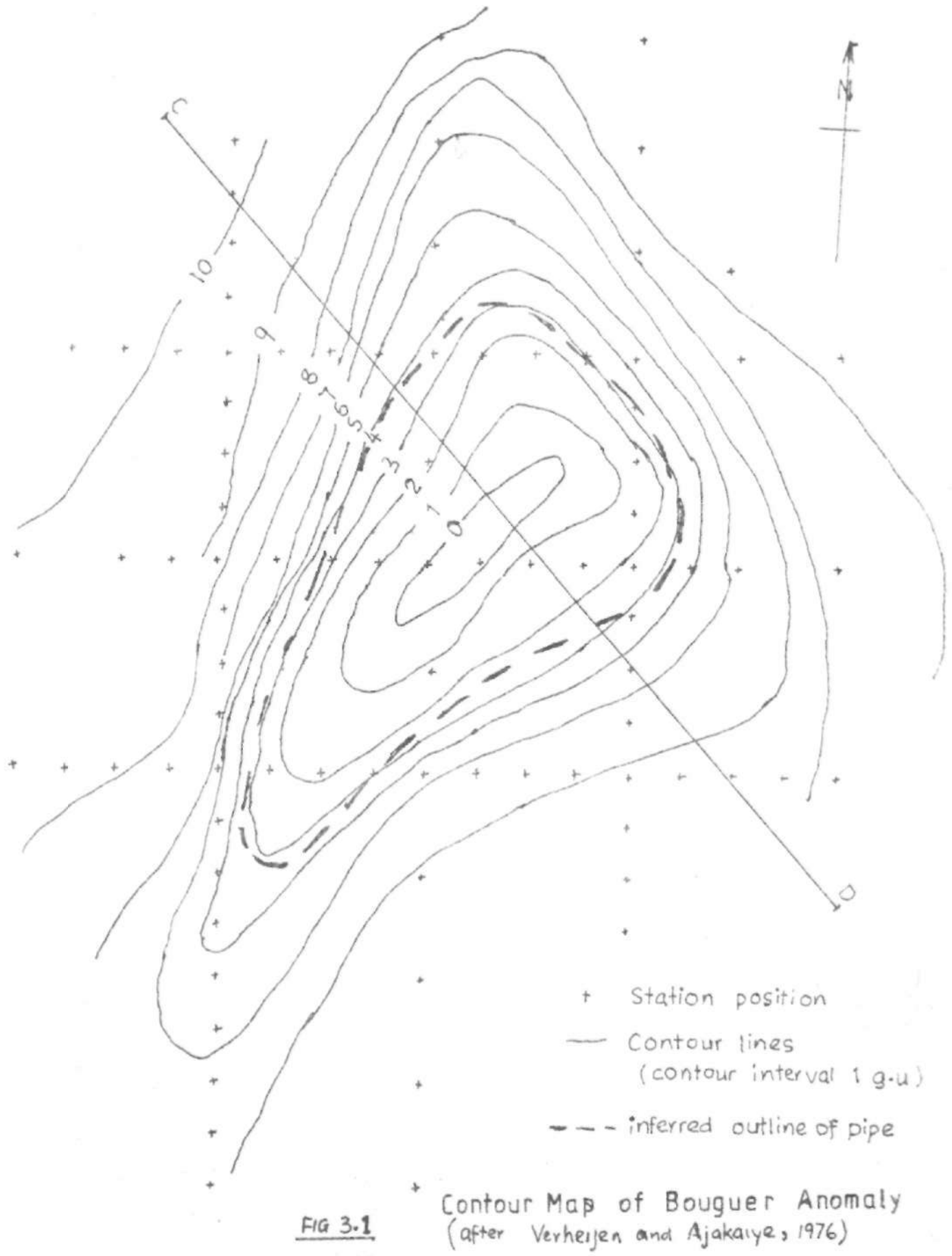


FIG 3.1 Contour Map of Bouguer Anomaly (after Verheijen and Ajakaiye, 1976)

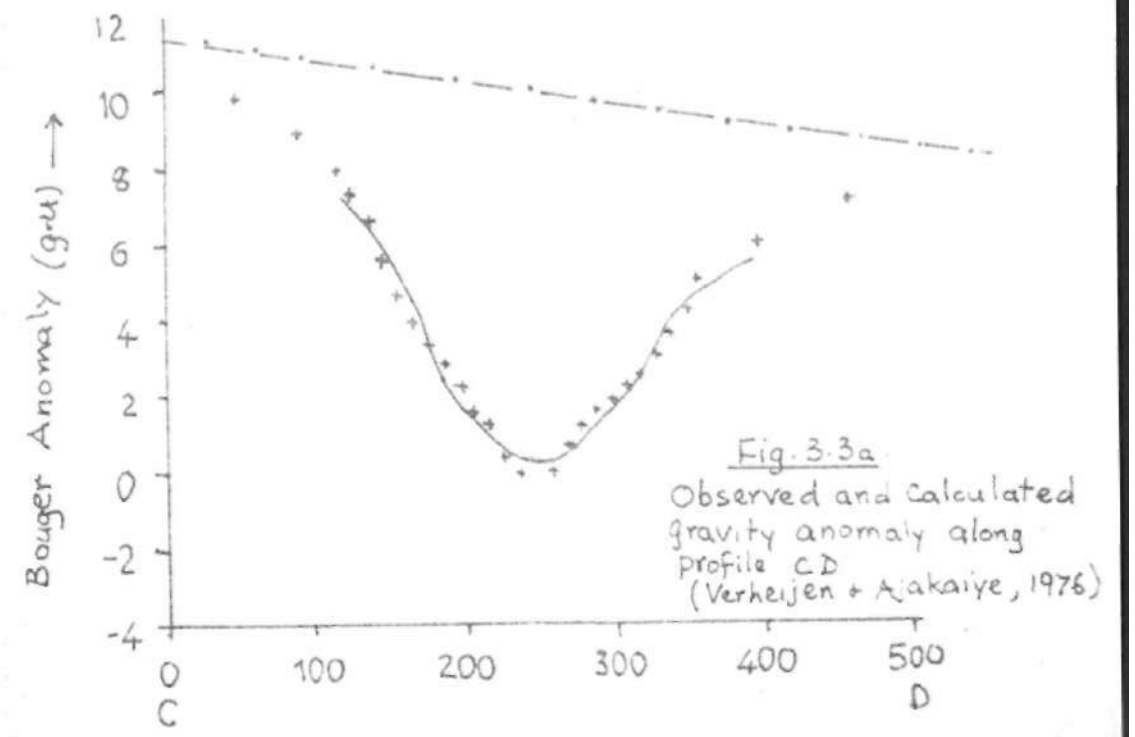


Fig. 3.3a Observed and calculated gravity anomaly along profile CD (Verheijen + Ajakaiye, 1976)

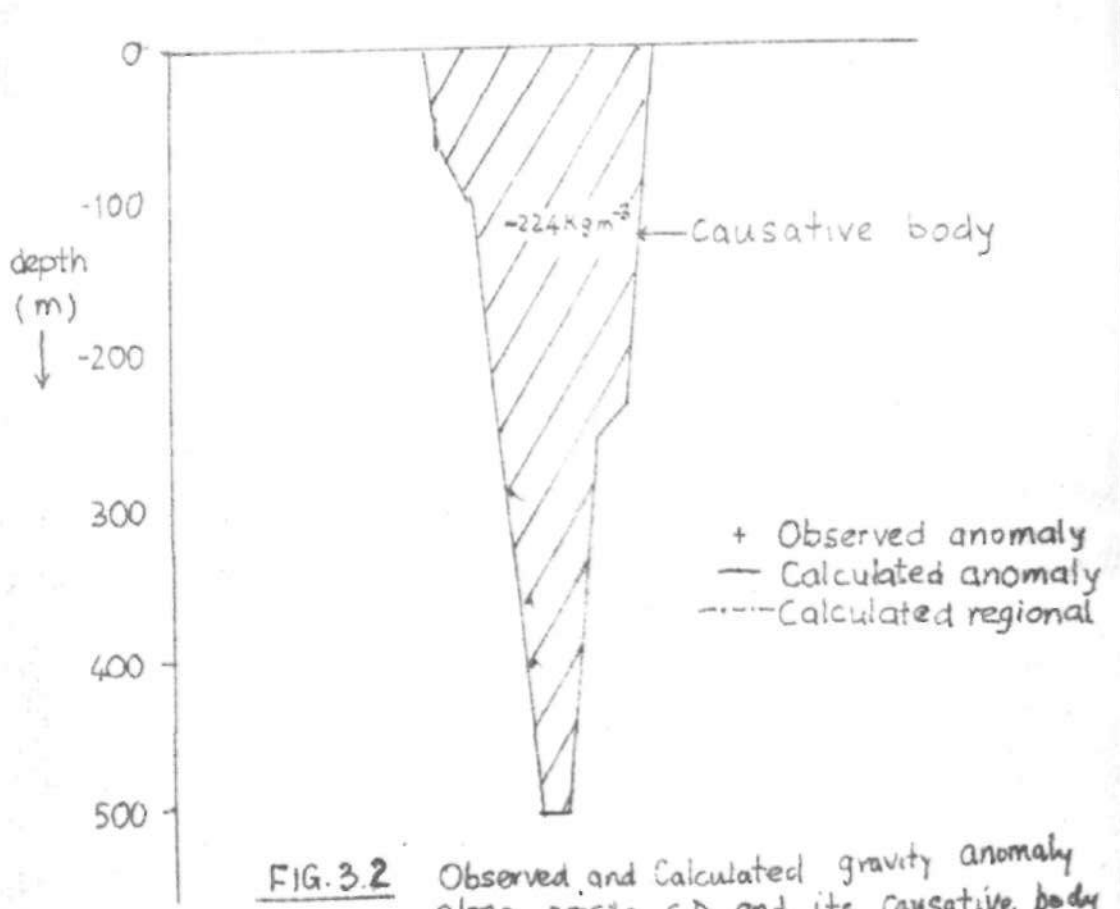


FIG. 3.2 Observed and Calculated gravity anomaly along profile CD and its causative body (after Verheijen + Ajakaiye, 1976)

A two dimensional analyses for the profile CD (fig. 3.1) was attempted, and a gravity model (fig. 3.2) was obtained. Fig. 3.2a suggests that a negative gravity anomaly was observed over the pipe. The calculated anomaly which gave the best fit to the observed was obtained by using a density contrast (between the surrounding and the intrusion) estimated at -224 ± 21 kg m^{-3}. This value falls in the range reported by Gerryts (1967). However, gravity method has been found to be often ambiguous when used alone (Paterson et al 1977). So it was fitting that other geophysical methods were used during the survey.

In the magnetic method a torsion magnetometer (Askania GFZ) was used to measure the vertical component of the magnetic field at the gravity stations. The reduced contour map, fig. 3.3 indicate an outline of the suspected pipe oriented in NE - SW direction. A profile along AB (fig. 3.4) was interpreted and the causative body found to be a dyke 130 ± 5 m wide, dipping at 90^{0}, with the surface at 12 ± 4 m depth. An estimated magnetic susceptibility of -36×10^{-3} S.I. units was reported. It was indicated that the model (fig. 3.5) did not produce a suitable fit to the observed curve. As a result it was speculated that the dyke which probably extended beyond the edges of the model might be dipping slightly inwards.

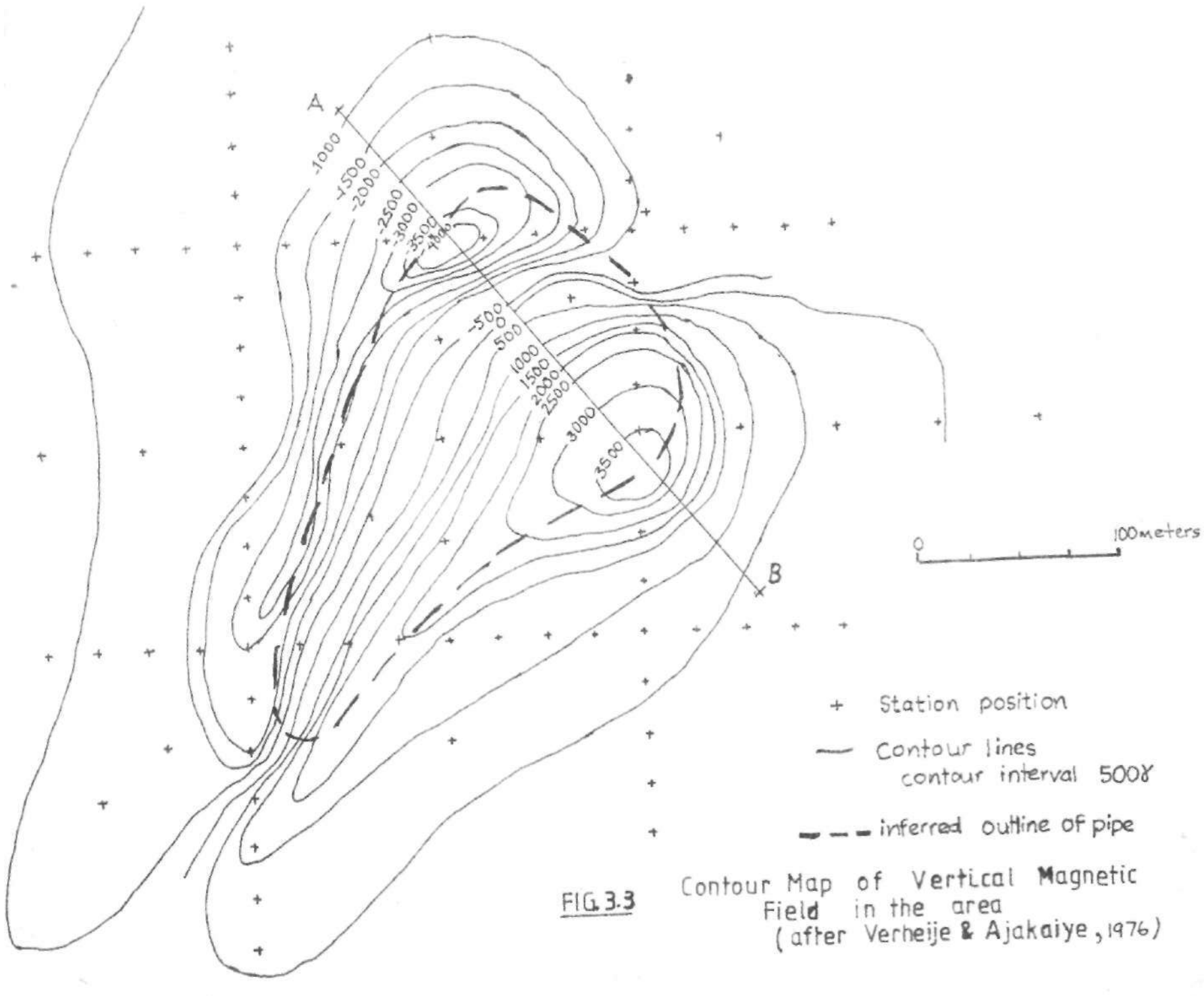


FIG. 3.3 Contour Map of Vertical Magnetic Field in the area (after Verheije & Ajakaiye, 1976)

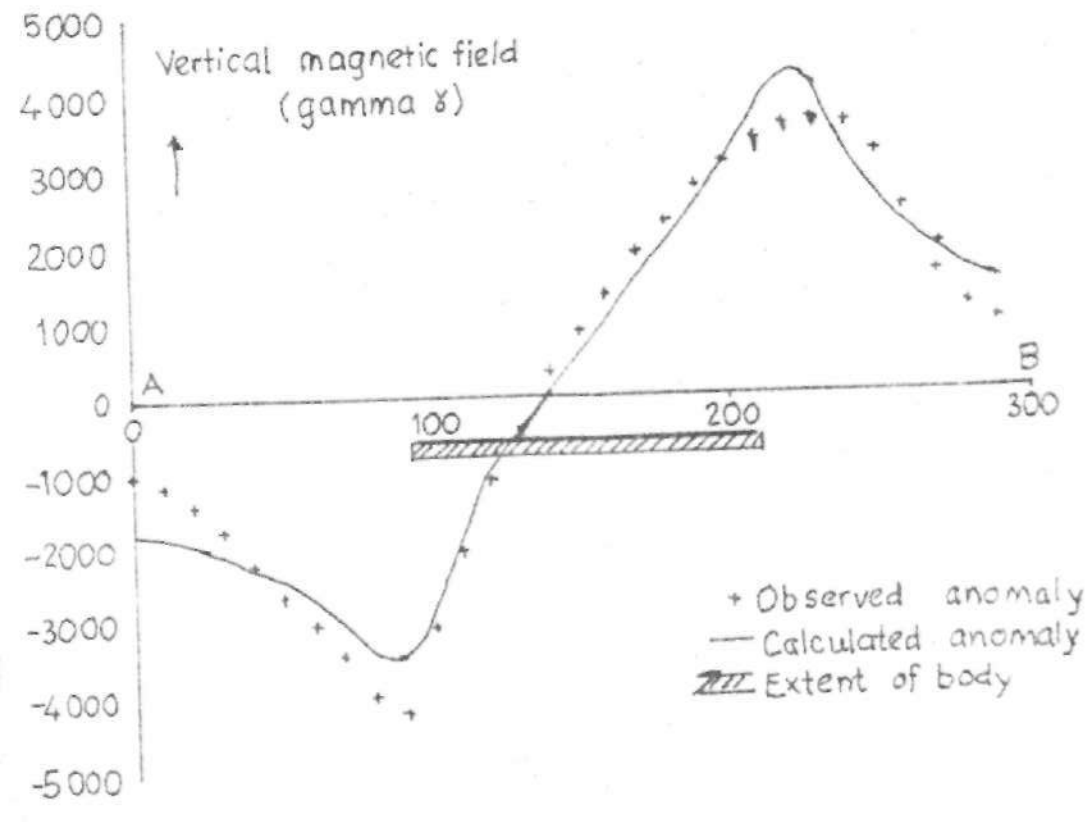


FIG 3.4 Observed and Calculated magnetic anomaly along profile AB (after Verheijen & Ajakaiye, 1976)

Again the magnetic low reported over the dyke compares favourably with Gerryts records for other places where magnetic method has been found successful. However the magnetic result was not conclusive since it appears a knowledge of the regional magnetic fields of the area was not indicated in the report.

The authors also carried out one Schlumberger electrical resistivity sounding with a single reversed seismic refraction spread near an anticipated centre of the pipe along CD (fig. 3.2). For the resistivity sounding an instrument (HEW-200) was used which could yield up to 1000 V/2000 mA and could measure a potential difference of the order of a few millivolts. For the seismic refraction measurements, a Huntec FS-3 equipment was used from which a penetration of 15 m into the ground was expected. Table 3.1 is the results of the combined interpretation of the seismic and resistivity sounding data.

TABLE 3.1

No.	Layer (m)	Seismic Velocity (m/s)	Resistivity (ohm-m)
1.	0 - 0.5	370	700
2.	0.5 - 3.6		15
3.	3.6 - 14	1400	15
4.	14 -	4300	750

Also, resistivity measurements using Wenner array was carried out along the same profile CD, and a resistivity low was reported over the pipe (fig. 3.6). The resistivity and seismic results were encouraging but they were very limited in coverage and nothing conclusive about the pipe can be deduced from them. Also, the gravity and magnetic field results, though they compare well with results reported by Gerryts (1967), were plagued with much ambiguity because a good knowledge of regional gravity and magnetic fields necessary for more objective interpretations were lacking. Thus it remains to accurately delineate the pipe and also to know if there are more pipes in the area since kimberlite pipes are known to occur in groups. Attempts have been made in the present report to throw more light on the issues. The methods of attack are discussed in the next chapter.

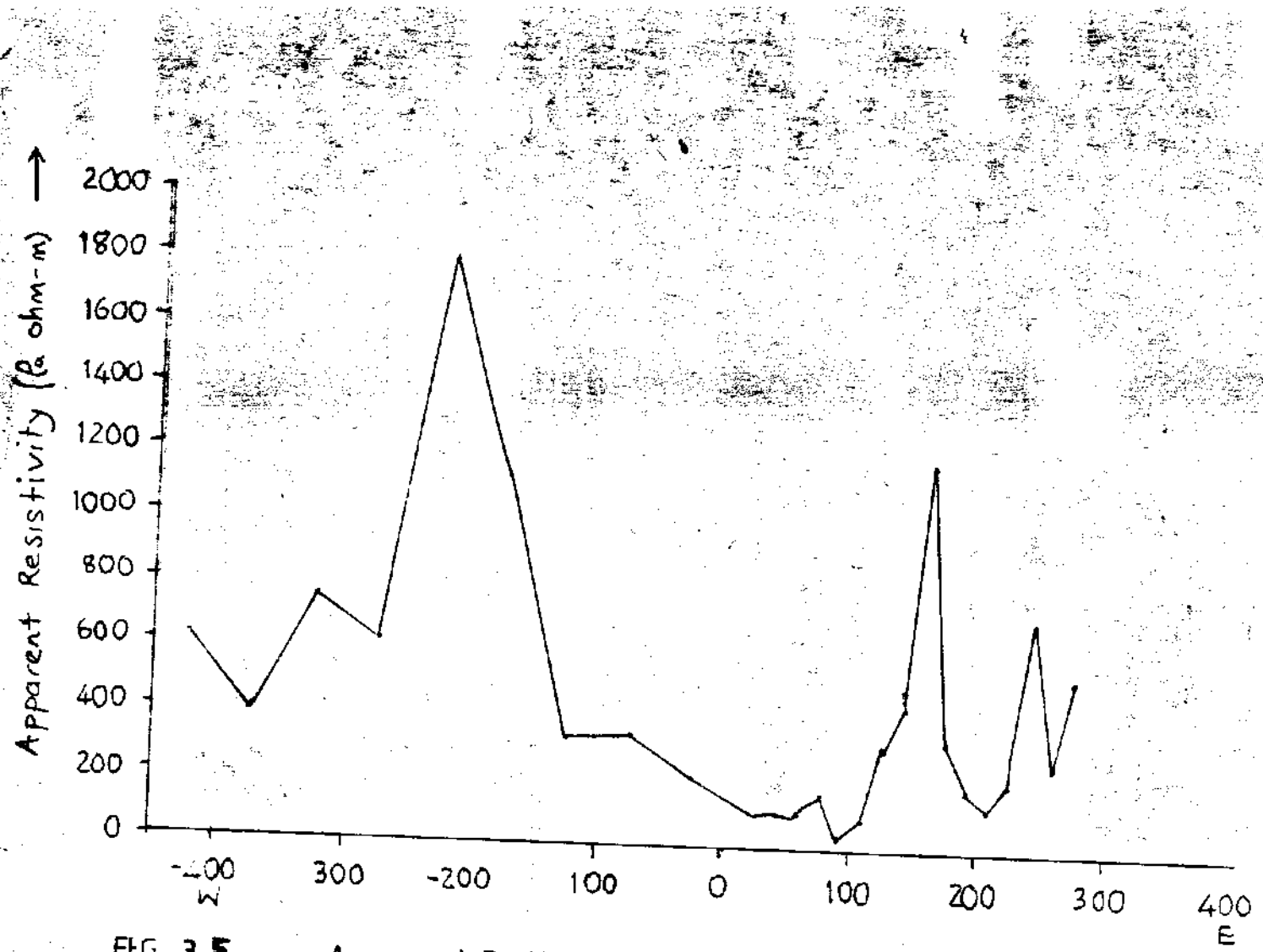


FIG. 3.5 Apparent Resitivity Profiling over the pipe
(from Veheijen and Ajakaiye, 1976)

C H A P T E R IV

THE PRESENT SURVEY, CHOICE OF METHOD AND FIELD TECHNIQUES

4.1 INTRODUCTION

The present survey is a detailed geophysical follow up of the work of Verheijen and Ajakaiye (1976, 1979) using the earths resistivity and seismic refraction methods. The survey is considered significant for the reason that a better delineation of the pipe will serve as a useful guide to both mineral and ground water explorationists since kimberlites are known to be associated with mineral deposits of economic significance and also considerable amount of water. The earth's resistivity and seismic refraction methods were employed because these methods have been used successfully in the location of kimberlite pipes in Bakwanga, Tanzania and Sierra Leone (Gerryts, 1967), as well as in Lesotho Central Africa (Peterson et al 1977). Both methods have also been successfully used in mineral and groundwater exploration programmes (Kollert, 1969). The choice of methods is discussed further in the next section.

4.2 CHOICE OF METHODS

It has been found that geophysical survey methods are required (in almost all cases) to accurately locate a kimberlite body when careful and proper interpretation of heavy mineral anomalies lead a prospector close to the kimberlite source. In cases where heavy mineral sampling methods failed, geophysical methods have been found successful in locating several pipes, for example in the Bakwanga diamond field in Zaire (Paterson et al, 1977). The choice of geophysical methods depends on physical characteristics of kimberlite and the difficulty often encountered is that kimberlite rock is reported to lack unique physical characteristics. However, magnetic, gravity, and resistivity anomalies have been reported over known kimberlite pipes (Gerryts, 1967 and Paterson et al, 1977).

During this survey the choice of resistivity and seismic methods was limited by such factors as the time available, the objectives of the survey and the geophysical methods already used during previous survey over the same body. The magnetic and gravity field methods were not used, partly because they had previously been used in detail over the same body and partly because of the reasons discussed below.

Even though the magnetic method proved effective in the discovery of several kimberlites in the U.S.S.R., ~~U.S.A.~~ and West Africa as reported by Gerryts, it was not equally successful in South Africa and Tanzania. In an attempt to explain the failure of the method, Paterson et al (1977) suggested that due to the effects of weathering and oxidation of a typical kimberlite, a sufficiently deep yellow ground (where it exists) could reduce the magnitude of the magnetic anomaly from the blue ground and the hardebark considerably, to the extent that the anomaly might not be distinguished from the background. It should be recalled that Turner (1975) and Verheijen and Ajakaiye (1976) accepted that the present intrusion is thoroughly decomposed. Also magnetic and gravity anomalies have no unique solution but can be explained by infinite number of models where drilling or geologic data are lacking (Parish J. B., 1978). The author is not aware of any drilling data that can be used for the present survey. More over gravity anomaly has been observed to be controlled by the surroundings - a positive gravity anomaly could be observed over fresh kimberlite with small negative near the peak where the body is weathered. And in volcanic rock surrounding it is reported that only the central gravity low corresponding to weathered or soft kimberlite

may be observed. For this reasons it was feared that gravity and magnetic methods already used may have not delineated this intrusion, in detail. Hence the choice of the resistivity and seismic refraction methods for this particular survey.

4.2.1 Resistivity Methods

4.2.1 (a) Introduction: Electrical resistivity methods can be used for obtaining quickly and economically the details and location, depth and resistivity of subsurface layers and is used widely in conjunction with seismic refraction method in prospecting for groundwater (Hasselstrom, 1968; Vingoe, 1972). The success of the method in the accurate mapping of bedrock or geologic boundaries of an instrusion, for example, depends on a good electrical resistivity contrast between the intrusion and the country rock. Lenox and Carlson (1967) condemn the use of this method in the determination of bedrock depths where sufficient control data (such as drilling data) are not available, as such depths may not be reliable. In the absence of any borehole control data in the area the method was used mainly to derive a picture of the distribution of the geologic formations within the surficial materials above the bedrock.

In an area where a kimberlite body is not exposed at the surface, Paterson et al (1977) have reported that the yellow ground on top of typical kimberlite ensures a resistivity low over the kimberlite irrespective of the resistivity of the surrounding formations. It has been found that the yellow ground has a typical resistivity of 20 - 40 ohm - m as against 100 - 300 ohm - m for porous sedimentary rock, 300 - 500 ohm - m for dry alluvium and 500 - 1000 ohm - m for basalt. Hence the resistivity method will be suitable for delineating the pipe in detail if the rock in the Kafur intrusion is a typical kimberlite pipe. Also the resistivity data in table 3.1 suggests that even though reliable depths or thickness of layer may not be obtained for lack of adequate control data (Lenox and Carlson, 1967) a picture of the distribution of geologic formations in the near-surface part of the suspected pipe may be determined.

Generally electrical resistivity method is based on the fact that different geologic formations may be characterized by different resistivities, so that when electric current is injected into the ground through two (current) electrodes, any subsurface variation in conductivity changes the current flow within the ground. This in turn affects the distribution of electric potential. The degree to which the potential at the

surface is affected depends upon the size, location, shape and conductivity of the materials within the ground (Vingoe, 1972). The potential difference is measured between another pair of electrodes (potential electrodes) placed in the line between the current electrodes. The ratio of the potential difference to the current is multiplied by a spacing factor to give the apparent resistivity, as a function of the electrode spacing.

The electrical conductivity of any geological structure depend on the conductivity of the rock formation its porosity, the water contained in the pore spaces and the salinity of the water. The most important factor is the water content. So the determination of the resistivity structure of the subsatum may reveal not only the geological structure but also the water bearing formations (Grant and West 1965; Vingoe 1972).

4.2.1 (b) Instrumentation and Measurements: For all electrical resistivity measurements in the present work the Geohmeter model 10, a Gish-Rooney type of electrical resistivity apparatus was used. The apparatus consists of the measuring instrument assembly, battery power supply and associated cables, reels and copper rods (electrodes). The measuring instrument assembly contained a current measuring circuit, potential measuring circuit, commutator and a reversing system. The assembly

was connected to the power supply through cables provided with plugs to prevent wrong connections. The flow of currents was determined by means of a multirange current milliammeter with a single scale reading (0 - 50) and a selector switch, which indicate the multiplication factor to be applied to the meter - reading.

The potential circuit include a galvanometer, potentiometer and circuit control devices which permitted the selection of any fraction of the total voltage for comparison and balancing against the potential difference being measured. The potential difference was determined by a "null" method, the instrument being designed so that no current flows in the galvanometer when the potentiometer output (in series opposition to the measured potential difference) was exactly equal to the input potential. The potential difference was then read in millivolts on the potential dials.

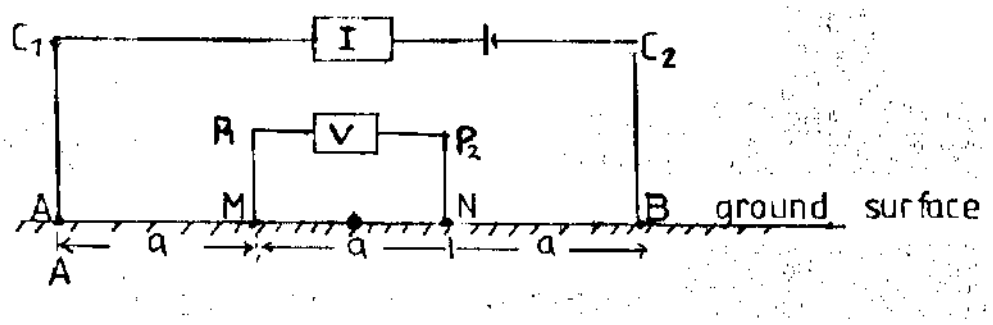
The instrument could yield as much as 180V/500mA between the current electrodes and measure potential difference of the order of $\frac{1}{1000}$ millivolts. Current was sent into the ground through two metal electrodes called current electrodes (C_1 C_2) while the resulting potential difference between another pair of electrodes (potential electrodes P_1 P_2) located inside the current electrode is applied to the input terminals of the

measuring instrument. The rotation of the commutator driven by a 12 volts storage battery periodically reverses the flow of the current to the external stakes C_1 C_2. A rheostat was used to control the speed of the commutator.

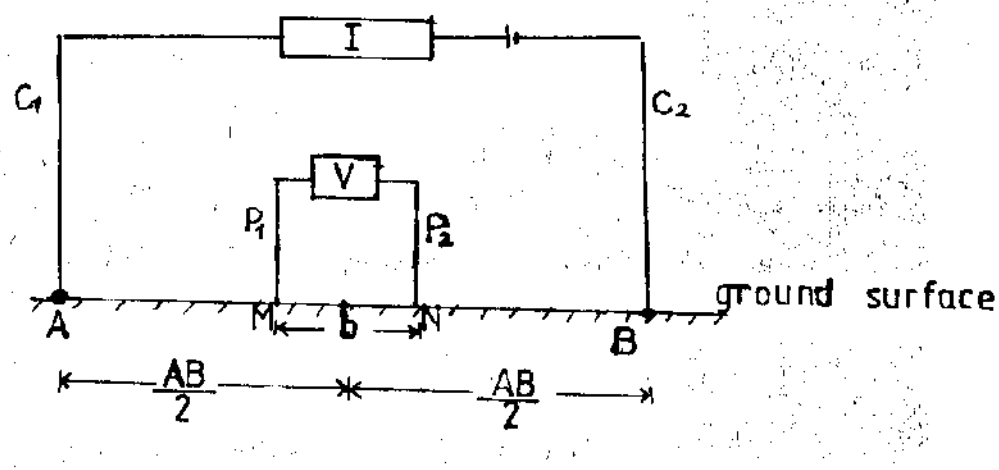
Two types of electrode arrangements were used for apparent resistivity measurements. They are the Wenner array and Schlumberger array shown in fig. 4.1.

In the Wenner array the spacing "a" between the four electrodes was kept constant as the whole array was moved along a profile and series of measurements at different location were taken at regular interval. Apparent resistivities obtained in this way as a function of the location of the centre of the electrode arrangement provided an indication of the lateral variations in resistivity structure at a given depth. This method of apparent resistivity measurement is known in literature as Electrical Resistivity profiling. It was used for reconnaissance survey for contacts and tracing of the boundary of the suspected kimberlite pipe.

In order to determined the spacing, a, between the electrodes an electrical resistivity depth sounding was performed at a reference station (described in section 4.3) to determined the vertical variations in resistivity structure. Vingoe (1972)



(ii) Wenner array



(iii) Schlumberger array

FIG 4.1 The Electrode Arrangements use for Electrical Resistivity Measurements

noted that a point of inflection on a resistivity depth sounding curve indicates the presence of an interface between two strata of different resistivities. An electrode spacing 'a' corresponding to the point of inflection would yield the best information for a particular depth under investigation. Based on an H-type sounding curve - obtained from the resistivity sounding - the constant spacings, a = 5 m and a = 20 m, were used to map the lateral resistivity variations near the top and bottom surfaces of the suspected kimberlite pipe along all the seven traverses (fig. 4.3) with Wenner electrode array. Each traverse was over 200 m long.

In the Schlumberger array the potential electrodes, P_1 P_2, (fig. 4.1b) were fixed at the centre of the line joining the current electrodes, C_1 C_2, while the current electrodes were moved symmetrically out-words. The two pairs of electrodes were symmetrically disposed about the midpoint of the array which was also the fixed observation station. As the electrodes expanded, the current penetrated deeper and the apparent resistivities measured at successively increasing electrode separation reflected the resistivity condition at larger depths (Parasnis 1966; Kunetz 1966; and Vingoe 1972). This method was used to detect resistivity changes and obtain informations

about thickness and apparent resistivities of subsurface layers where enough resistivity contrasts existed between the layers.

The Schlumberger electrode array was preferred because of speed and the effect of local inhomogeneity. Only two electrodes are moved so that the field procedure was quicker than would be the case if the Wenner method was used. Also the potential electrodes were kept 'fixed' so that the effect of local shallow inhomogeneities near them were kept constant for all measurements. In actual practice it was necessary from time to time to increase the potential electrode spacing (P_1 P_2) in order to obtain a potential difference large enough to be measured with satisfactory precision. P_1 P_2 (= b) was increased in such a way that its value was 10 - 20% of the current electrode spacing (A_1). The values of b and the corresponding value of $\frac{AB}{2}$ were chosen in order to obtain overlapping readings whenever a change over of b from one value to another was made.

4.2.2 Seismic Refraction Method

4.2.2 (a) Introduction: Seismic refraction method has been described as a reliable and economic method of determining depth-to-bedrock (B. Hasselstrom; 1968) and the method has been widely used in conjunction with resistivity method in water and mineral exploration and in engineering geophysics such as foundation studies. It has been useful in the location of more or less vertical fissures, contact and fault zones, some of which serve as channel for the transportation of groundwater to lower levels; and in the determination of the thickness of near surface weathering layer and for bedrock surface mapping. It has often been used to determine subsurface elevations of various layers within the overburden (Hawkins, 1961; Hagedoorn, 1959; Morley, 1967; Green, 1973; Dobrin, 1976; and Telford et al 1976). Green pointed out that the method has been most successful in exploration and engineering applications when applied to shallow depths (of about 100 m) problems in areas that were geologically not too complicated. However its application in the delineation and investigation of kimberlite pipe elsewhere is not known to the author. Nevertheless this method was employed during the present survey to assist resistivity methods in the location and study of the contact

zones between the intrusion and the country rock, to determine the thickness of weathering of the intrusion and the various layers in the overburden.

The application of seismic refraction method is based on the principle that different earth layers (assumed horizontal) have different propagation velocities for seismic) seismic waves and that such velocities increase with depth, the velocity of the lower layer being higher than that of the layer above it. The method requires that at every interface or geologic discontinuity the velocity changes abruptly (Kanges T. 1963). This however was not always the case met in field practice (see next chapter).

4.2.2 (b) Instrumentation and Measurements: An ABEM - TRIO seismic refraction system, type 5352, was used for the data acquisition. The instrument is a multichannel battery driven seismic refraction system. It measures seismic velocities by detecting vibrations produced by artificial energy source. Two sticks of explosives (gelatine dynamite 80% strength) were used at each shotpoint as the energy source. The explosives were buried about 0.5 m below ground surface in hand augered holes so that waves generated could penetrate deep into the ground from where they could be reflected or refracted at

different rock interfaces. The refracted waves were detected by a set of twelve geophones located on the ground surface at different distances from the energy source. The geophones were connected through a cable to the seismograph where the arrivals of seismic waves at each geophone were recorded on a dry-write recording paper. The spikes of the geophones were buried so as to increase the signal to noise ratio and reduce the effect of noise from wind around the seismometer.

Fig. 4.2 illustrates the geophone layout on each spread of 110 m length. Five shots were fired for each geophone spread. These consisted of two end shots, two long shots, and one centre shot. The end shot located at either end of the spread were each at a distance of 5 m from the end geophone; the long shot were located as above at distance of 40 m from the end geophone, and the centre shot was located at the centre of the geophone array with six geophones on either side of the shot point and displaced 1 m off the line of geophones. As the shots were fired one after the other, the recording instruments remained in fixed positions so that conditions under the geophones remained unchanged. Under such situations changes in the arriving waves are considered very important. Sander and Overton (1965) indicated that such changes imply that the waves travelled along different refraction paths.

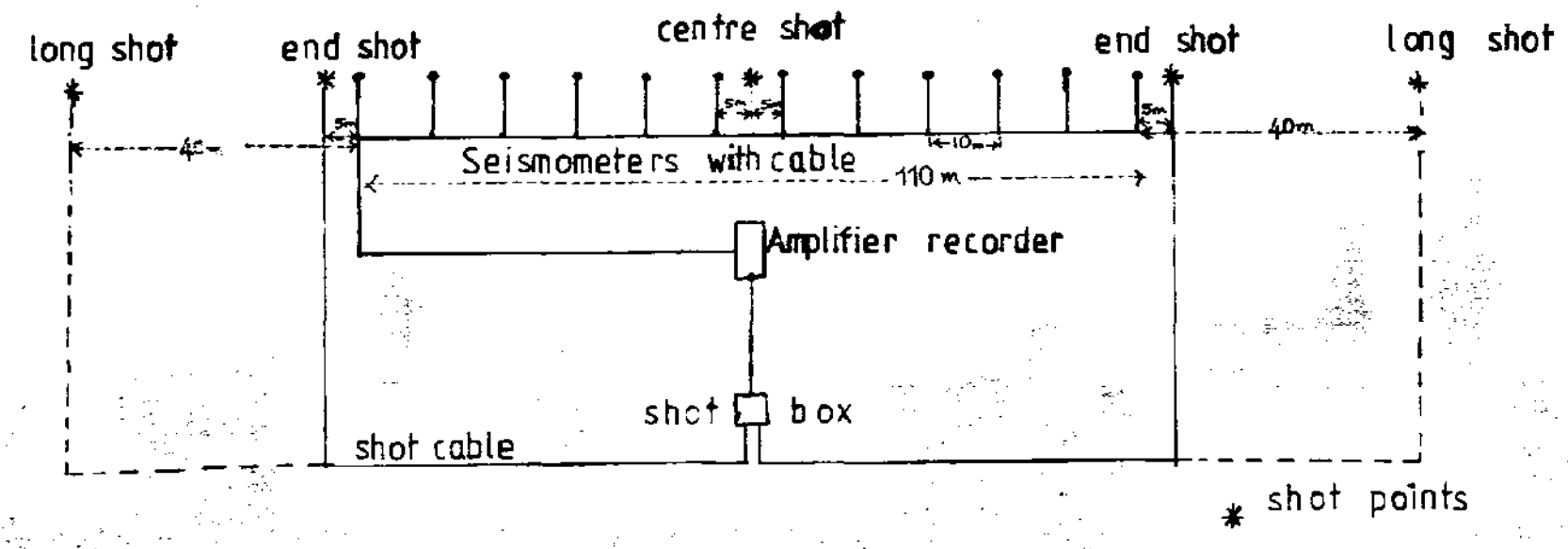


FIG. 4-2 Field set-up of TRIO System

The end shot and centre shots were needed for more accurate determination of velocities and thicknesses of near-surface layers, while the long shots were used to provide detailed information about deeper layers. Continous profiling method was adopted, with adjucent spreads over-lapping one geophone station.

The time distance curves for each spread were plotted and the velocities and depths of refractors were determined using the "Plus-Minus" method and the Reciprocal Time method, as detailed by Hagedoorn (1959) and Hawkins (1961), respectively. The curves and their interpretation are treated in detail in the next chapter.

4.3 FIELD TECHNIQUES

The field operations were designed to cover as much of the kimberlite body as practicable within the limited time available. A total of 26 days were spent in the field between November 1978 and March 1979. The survey team consisted of the author, three field assistants - two of whom were employed locally. During the seismic survey the team was expanded to include a technician and two other assistants.

Before the field measurements were commenced, two trips were made to Massari in an attempt to locate the site. On the

basis of the available information on the suspected kimberlite and the flat topographic relief of the area, a grid pattern was adopted for the field network. An open pit suspected to be situated on the suspected pipe was chosen as the reference station in the absence of a bore hole or bench mark in the area. The presence of scattered grains of ilmenite around the pit prompted the choice of the pit as the reference station. A base line Y_0 over 800 m long and running NE - SW was defined through this reference station (Fig. 4.3). The SW section of the baseline terminates in a settlement, Gida dan Tanko.

Six cross traverses each over 200 m long and running NW - SE were chosen to intersect Y_0 at 100 m intervals. They were labelled X_0, X_1, X_2..., X_5 (fig. 4.3). The X_1 traverse crosses Y_0 at the pit. For easy location, each point on the NW - SE (cross-traverse) was identified by its position NW or SE of Y_0 while stations on Y_0 were identified by their locations NE or SW of the pit.

Resistivity profiling measurements using Wenner arrays were carried out on all traverses while seismic refraction survey was conducted on baseline Y_0, X_1, and X_5 (Fig. 4.3). Continuous profiling method was used with one overlapping geophone station to cover distances of 500 m on Y_0, 430 m on

Masavi/Kafur

N

45° NE

MIN SX

to Gide

dan Tanko

BASELINE (Yo)

VES H

VES G

VES C

VES F

VES E

VES B

VES D

VES A

PIT (ORIGIN)

Kafur

XE

X5-SE

X4-SE

X3-SE

X2-SE

X1-SE

X0-SE

0 20m 40m

KEY

- outcrops
- foot paths
- resistivity profiling line
- •VES resistivity sounding point
- seismic refraction traverse
- outline of pipe

FIG.43 GEOPHYSICAL SURVEY MAP
(showing outline of pipe at 20m depth)

C H A P T E R V

INTERPRETATION

5.1.1 RESISTIVITY PROFILES

The first resistivity profile on the site was the reconnaissance survey along the Baseline, Y_0 traverse, to detect the suspected kimberlite intrusion. The profile was designed to cross the pit (fig. 4.3) which was the only pointer to the location of the intrusion at the beginning of the survey. The result is given in fig. 5.1, with the pit (the reference station) located at Y_0, 00. Also resistivity profiles were measured along six traverses which cross Y_0 at 100 m intervals, The results of these are shown in fig. 5.1 to fig. 5.6. In the following sections the profiles on all traverses are discussed first on the bases of their common features after which the profiles along the six parallel traverses and the one along Y_0 are treated separately.

5.1.1a Resistivity Profiles - Common Features

A close examinations of all the curves reveal possible contact regions (at, e.g., near Y_0 80 m NE and Y_0 220 m SW, see fig. 5.1) between low resistivity blocks and formations with

much higher apparent resistivities. The contact zones are characterised by sharp resistivity gradients and fairly uniform apparent resistivity values on either side of the contact. The contact zones may be steeply dipping in the direction of the low resistivity block.

The apparent resistivities obtained with both electrode spacings correlate well in most cases although generally the width of the low resistivity blocks on each profile is bigger for a = 20 m than for a = 5 m. The variation in the width of the anomaly may be attributed to variations in the thickness of the overburden. Where the top of the low resistivity body is shallow apparent resistivities from both spacings are very close.

Substantial scatter is observed in the a = 5 m curves. Such erratic behaviour may be due to near-surface inhomogeneities or lack of sharp resistivity discontinuity at the 5 m level due to variations in overburden thickness or both. The discontinuities on both curves close to the edges of the contact zones could be due to the discrete nature of the four electrode locations with respect to the contact. Each time one of the four electrodes (Wenner array) crosses the boundary between formations of different resistivities, this appears

as a discontinuity (Keller and Frischnecht, 1977).

A close look at elevation and resistivity curves indicates that the effect of surface topography on the resistivity profiles if it exists, is not significant. It can further be observed on all curves that over the higher resistivity regions outside the diatreme the apparent resistivity values with a = 20 m are higher than the apparent resistivities for a = 5 m. The implication is that there the surrdunding basement is very near to the surface.

5.1.1b Apparent Resistivity Profile Along Y_0

The resistivity profiles along Y_0 were as given in fig. 5.1 On both the 5 m and 20 m spacing curves, sharp resistivity gradients can be observed near Y_0 80 m NE, and 100,210 and 520 mSW. The sharp gradients indicate locations of contacts between low resistivity troughs and the higher resistivity formations flanking the troughs. On closer examination it can be observed further that the discontinuities in the 5 m spacing curve are sharper than those for the 20 m spacing curve, at the contacts.

Three main troughs can be identified on the 5 m curve as against two on the 20 m curve. What appears like ripples or noise on the 5 m curve may be attributed to local near-surface

inhomogeneities and measurement fluctuations. The discrepancy between the two curves may be due to variations in the thickness of a resistive overburden and near-surface inhomogeneities as well. Where the thickness of the top layer exceeds about 5 m high apparent resistivities (greater than 50 ohm-m) will be measured.

In the neighbourhood of the pit, about Y_0 00, the low apparent resistivities (5-20 ohm-m) suggest presence of wet clay/ilmenite. The presence of ilmenite around the pit and the low resistivity observed around the pit suggest that the pit was situated on the suspected intrusion. If the material with the low resistivity contain clay, the clay may be associated with the intrusion as should be expected in a kimberlite pipe (Garrytø, 1967; Paterson et al 1977).

By comparing curves on either side of the resistive region between Y_0 120 and 210 SW it may be suggested on the basis of low apparent resistivities (of the order of 10-20 ohm-m) that the low resistivity formations are probably part of one and the same suspected kimberlite pipe.

The cause of the rapid fall in the "20 m" curve between Y_0 400 and 510 m SW is difficult to explain. Apparent resistivity as low as 2.0 ohm-m was measured at 490 m SW. It may be associated with highly saline ground water or an increase in water content.

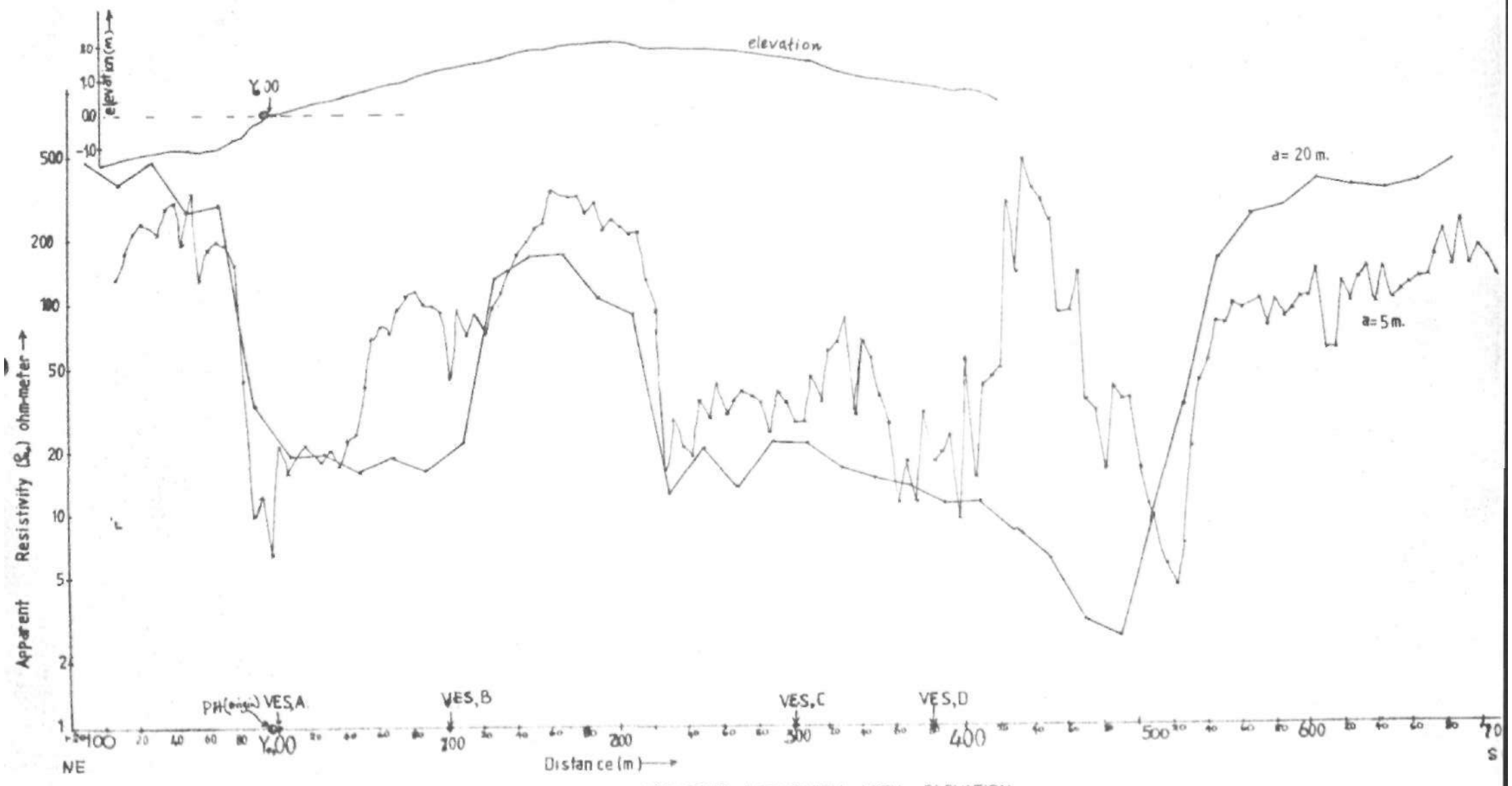


Fig 5.1 APPARENT RESISTIVITY WITH ELEVATION
showing sounding points (V.E.S)

5.1.1c Profiles Along X_0, X_1,---, X_5 Traverses

These six traverses run in NW-SE direction across the baseline Y_0 at 100 m apart and each traverse, over 200 m long, extends across the whole width of the low resistivity blocks. Resistivity profiles along the traverses were performed to locate the boundaries of the low resistivity formation detected along Y_0. The profiles in figs. 5.2 to 5.7 were obtained. They have been found to have identical features with profiles along Y_0. (Section 5.1.1a) A closer look at the profiles reveal few differences, in the width of the low resistivity blocks and the values of the apparent resistivities on the flanks of the low resistivity blocks. The width decreases southwards as shown more clearly by the contour maps fig. 5.8 and fig. 5.9. On the flanks of the anomalous (low resistivity) body the high apparent resistivities (Pa greater than 300 ohm-m) coincide with the locations of basement outcrops along the traverses. The apparent resistivities fall in the range for granite rocks (Table 5.1), and this is consistent with the local geology of the area.

On traverse X_0 the two curves do not agree very well, because the resistivity lows on the 5 m curve are not well defined on the 20 m curve. The low resistivities may be due to near surface inhomogeneities. At X_0, 80 m NW, the situation

may be different. The anomaly at this location may have a deeper origin and the source may be a thin vertical dykes probably too thin to be detected with the 20 m electrode spacing. Beyong 100 m NW thick vegetation prevented further profiling. Hence the behaviour of the curves beyond that location could not be determined.

On each of traverses X_1, X_2...., X_5 the size of the anomalies obtained with 5 m and 20 m constant electrode spacings are different. On traverse X_3 (fig. 5.5), for instance, the width of the low resistivity block is smaller on the 20 m curve than on 5 m curve. The anomalous body is probably smaller in size at 20 m than at 5 m depth.

It could further be observed (in fig. 5.5) that the apparent resistivities at 20 m spacing between stations on X_3 at 20 m and 70 m SW, are relatively higher than the values obtained at 5 m spacing between the same stations. Keller and Frischknecht (1977) have noted that such changes indicate changes in the water content or salinity (between the two depths mapped).

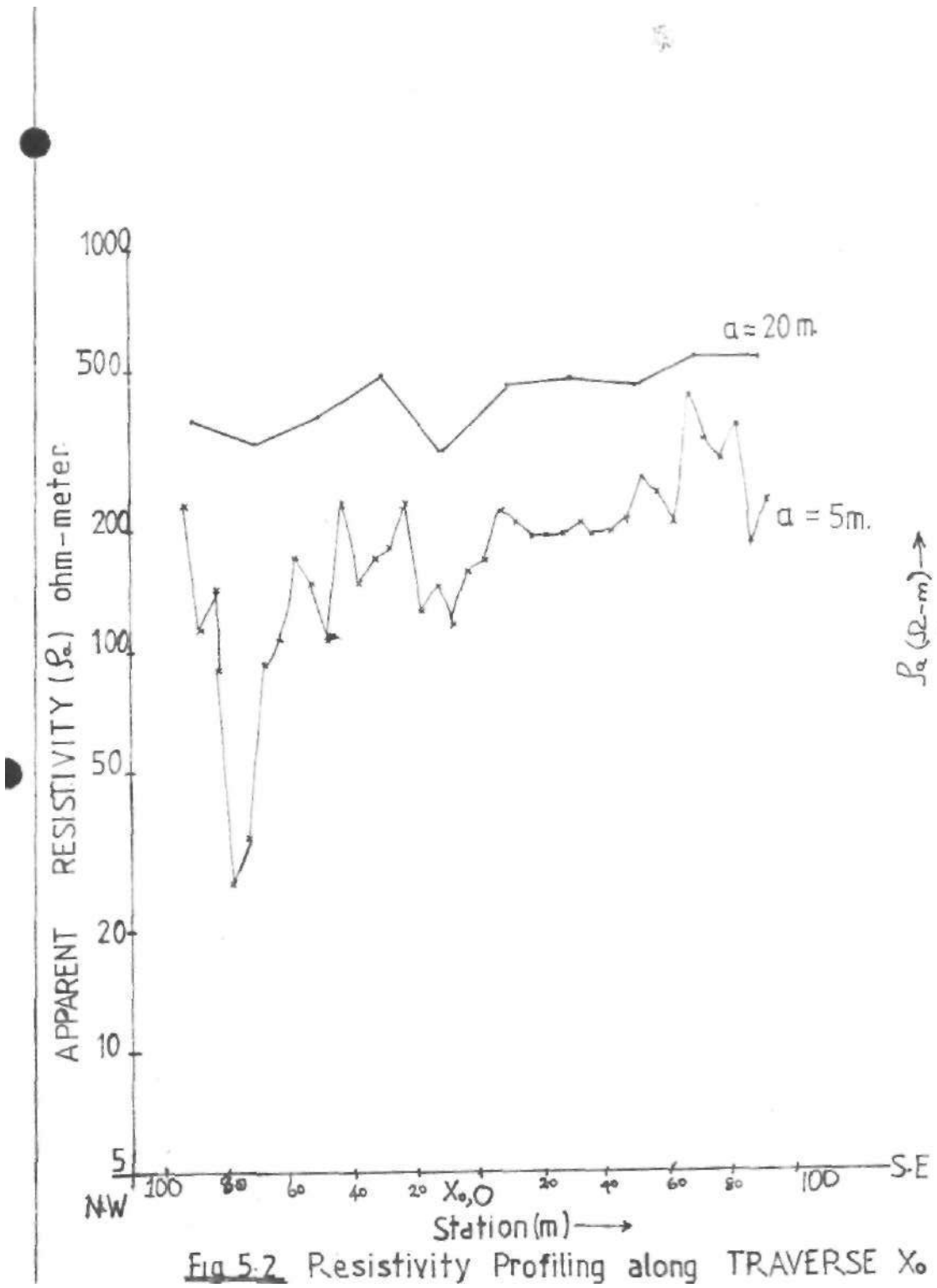


Fig 5.2 Resistivity Profiling along TRAVERSE X_0

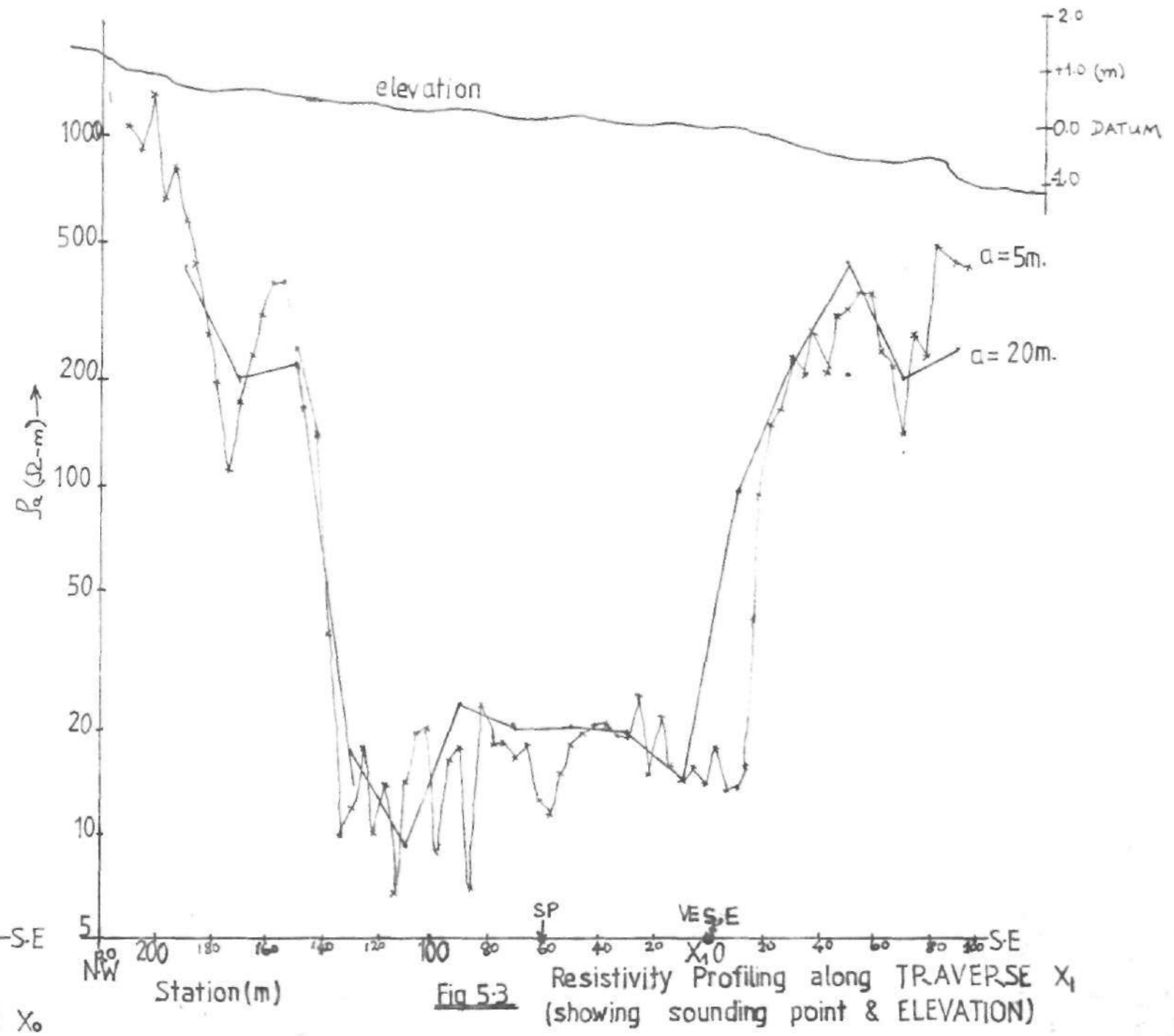


Fig 5.3 Resistivity Profiling along TRAVERSE X_1 (showing sounding point & ELEVATION)

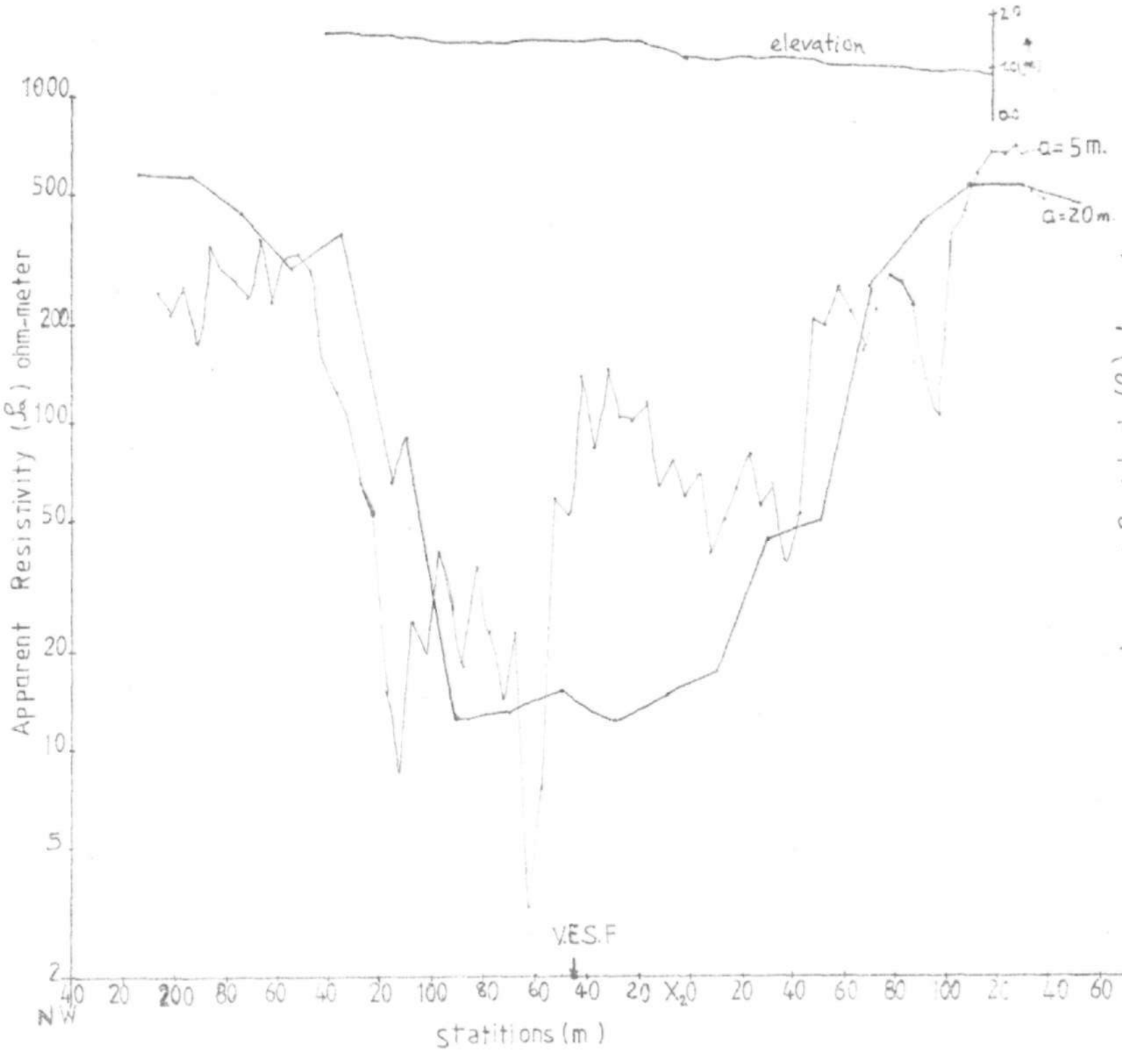


Fig 5·4 Resistivity Profiling along TRAVERSE X_2 (showing Sounding Point & ELEVATION)

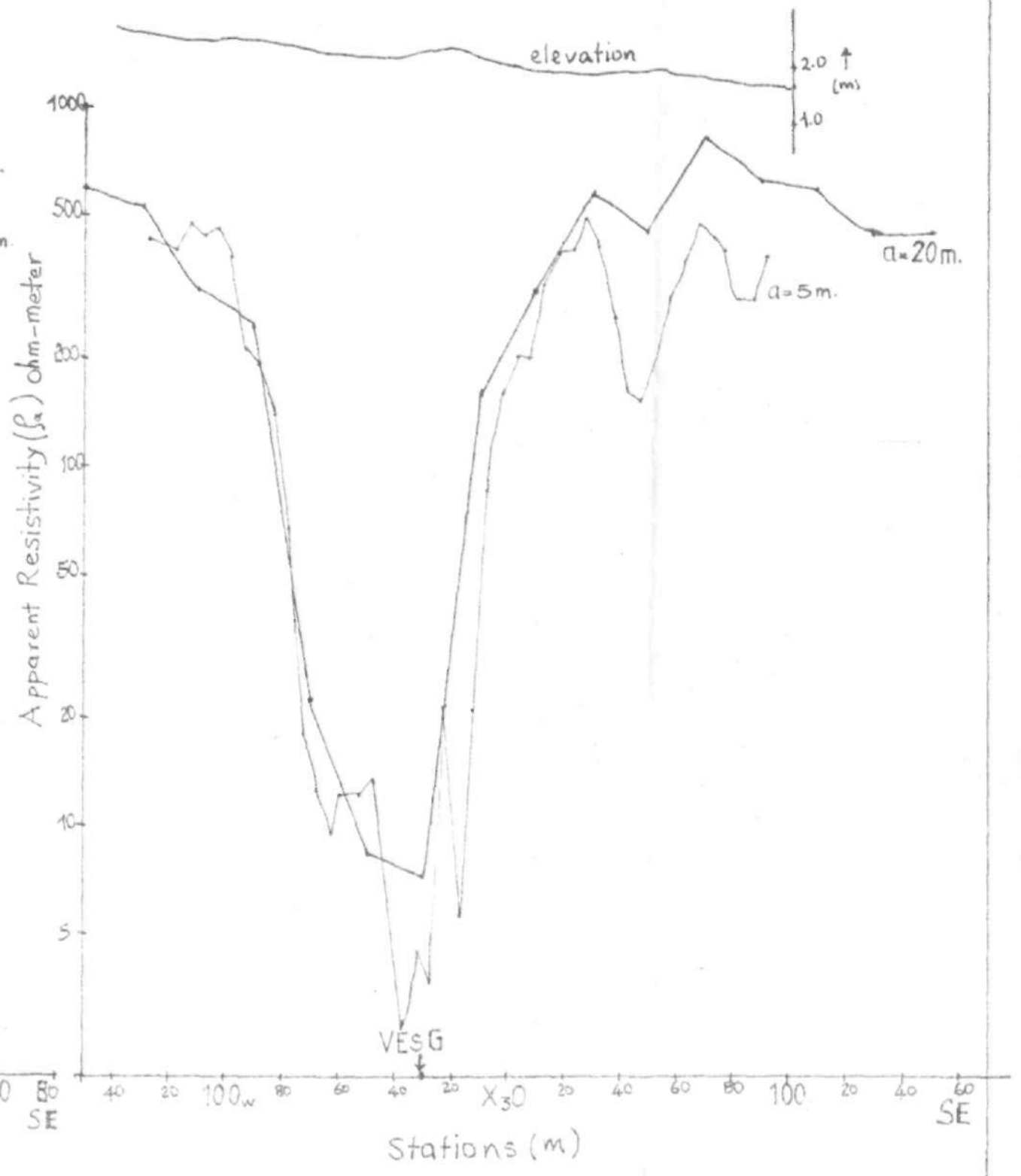


Fig 5·5 Resistivity Profiling along TRAVERSE X_3 (showing Sounding Point & ELEVATION)

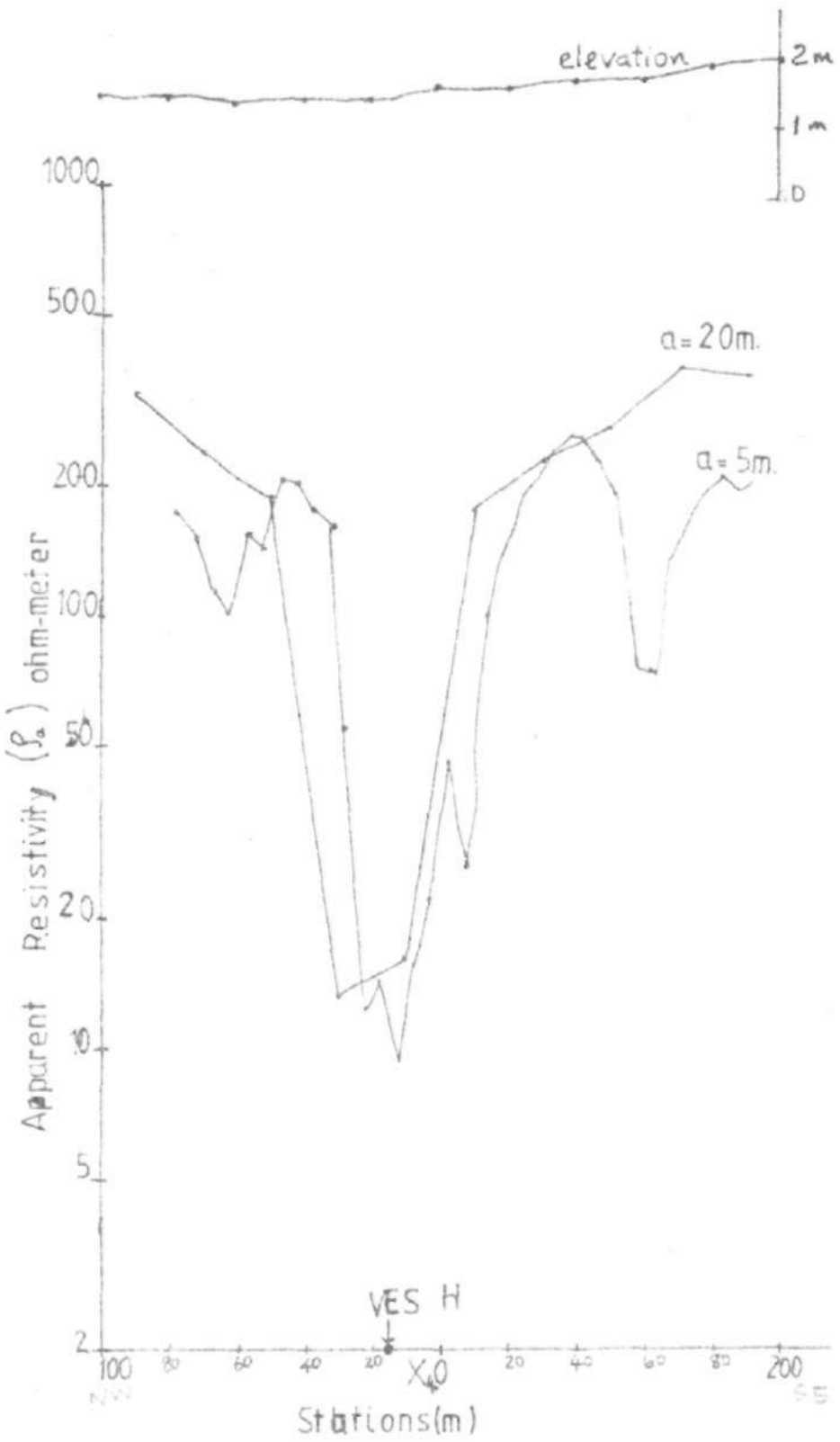


Fig 5·6 Resistivity Profiling along TRAVERSE X_4 (showing Sounding Point & ELEVATION)

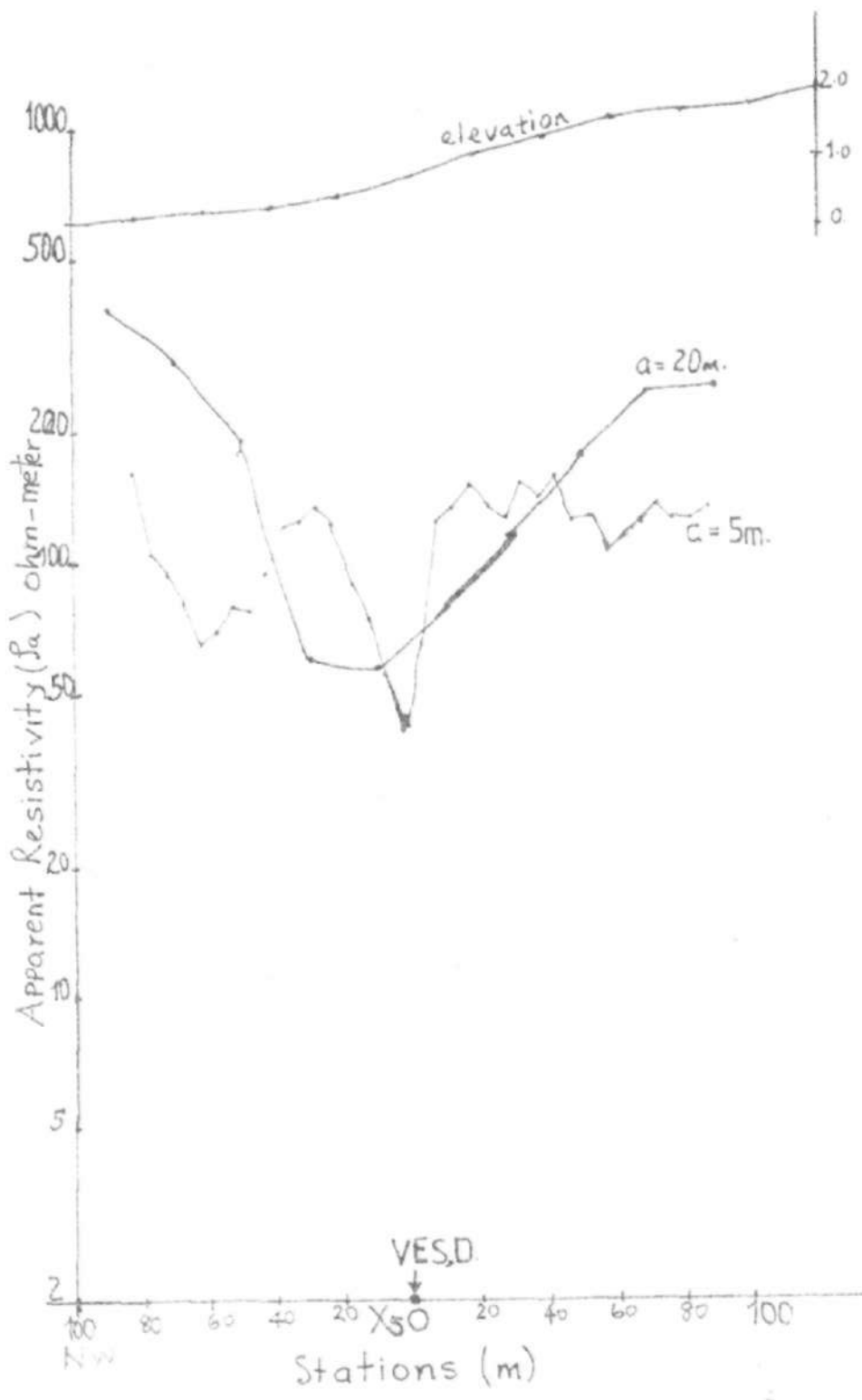


Fig 5·7 Resistivity Profiling along TRAVERSE X_5 (showing Sounding Point & ELEVATION)

5.1.1d Results

The results of the resistivity profilings on all the traverses have been represented in form of two apparent resistivity contour maps as in fig. 5.8 and fig. 5.9 for spacings a = 5 m and a = 20 m respectively.

On both maps the outline of the boundary between the suspected kimberlite pipe and the country rock has been defined by 50 ohm-m contour line. The pipe is suspected to lie within the shaded area, where apparent resistivity values less than 50 ohm-m were obtained. The results suggest that the pipe is between 560 and 660 m long, with a geoelectric strike oriented in a direction east of NE. It is widest in the northern part between the pit and X_2 traverse. The width decreases southwards from a maximum value of about 140 m between X_1 and X_2 to about 20 m on X_5, and probably less than 20 m between X_5 and Gidan dan Tanko to the South.

Based on the resistivity profiling results, five resistivity sounding points were sited on the geoelectric strike at 100 m interval, as in fig. 4.3, to investigate the variations in the geoelectric sections in the pipe. Four other sounding points were located and Y_0 so that resistivity sounding results could be compared with seismic refraction results. The seismic refraction spreads were laid out on the bases of resistivity

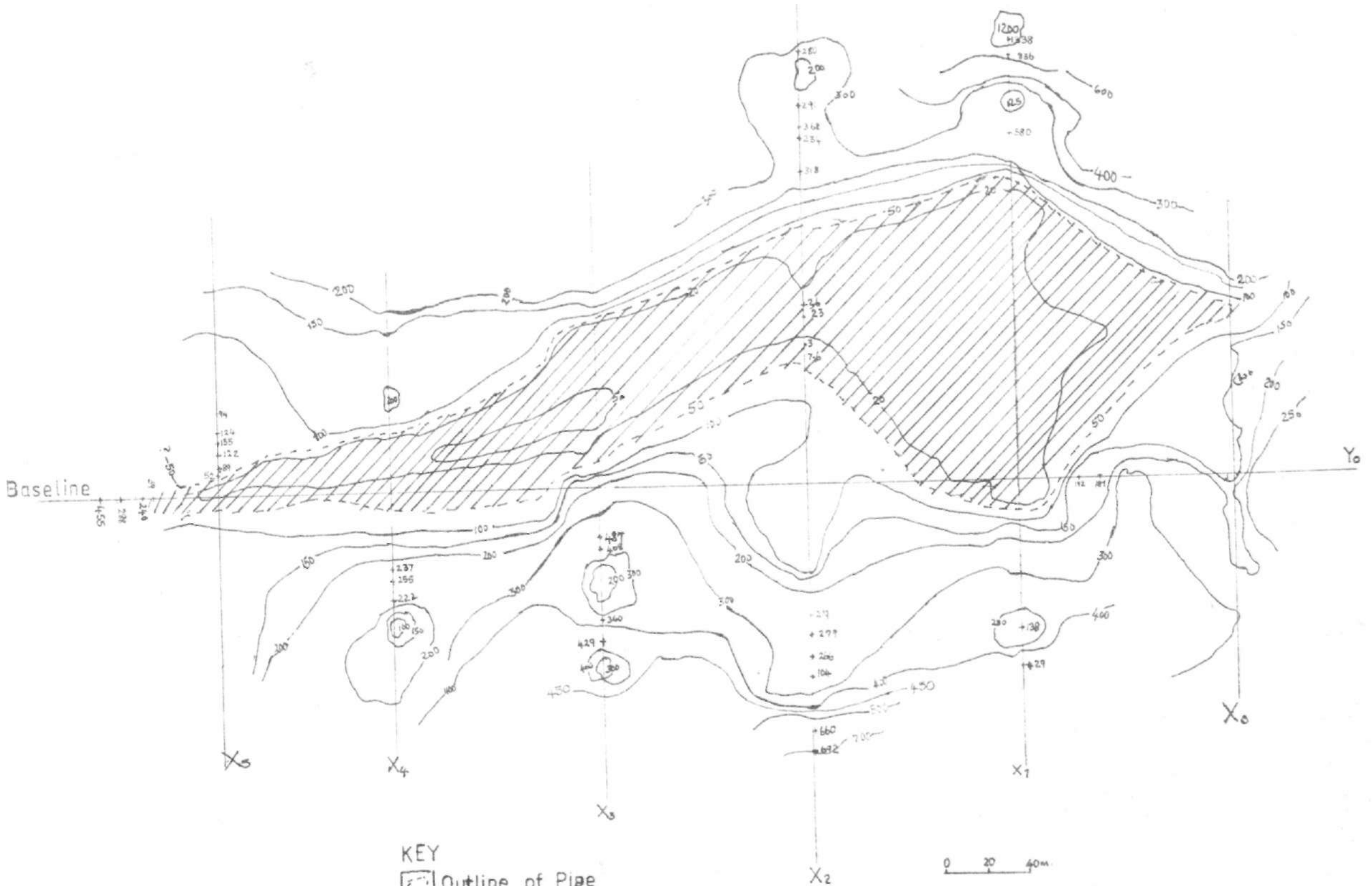


FIG. 5.8 APPARENT RESISTIVITY CONTOUR FOR 5m ELECTRODE SPACING

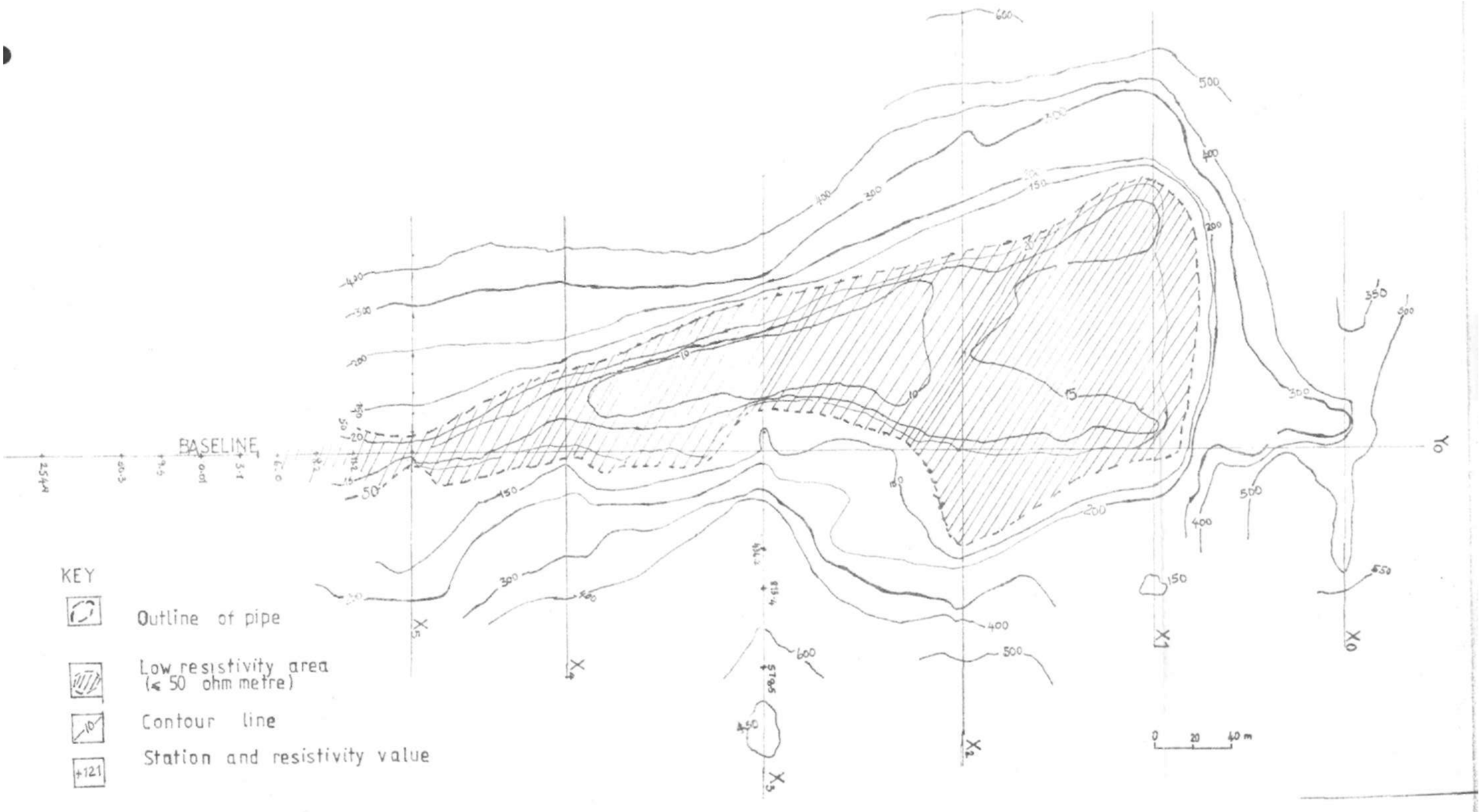


FIG. 5.9 APPARENT RESISTIVITY CONTOUR FOR 20m ELECTRODE SPACING

profiling results, with the aim of using the refraction results to supplement the profiling results on the location and the nature of the contacts between the the pipe and the country rock.

5.1.2 Vertical Electrical Soundings

With the Schlumberger array used for the electrical resistivity or vertical electrical (VES) the apparent resistivities were calculated using the relation.

$$a = \left(\frac{s^2}{b} - \frac{b}{4}\right) \frac{V}{I},$$

Keller and Frischknecht (1977)

where
- s = half current electrode spacing
- b = potential electrode spacing
- V = potential difference measured between the potential electrodes
- I = the current put into the ground.

The results of the electrical soundings were presented in graphs in which half the current electrode spacing was plotted on the abscissa and the corresponding apparent resistivity was plotted on the ordinate. The scales on both axes are logarithmic. One advantage of the logarithmic scale is that it facilitate comparison of the field curves with theoretical master-curves

pre-constructed on bi-logarithmic scales.

Qualitative interpretation of field curves were made to identify the number of layers and the approximate parameters of the geoelectric section. Except for two locations three layer H-type of curves were obtained at all sounding points. For reasons given later, VES C and VES G could not be interpreted. All curves were observed to be characterised by a final segment of positive gradient which in some cases approach 45 degrees. This indicates a highly resistive bottom layer. Substantial amount of scatters were observed on all curves at large spacings. At sounding points where cross soundings were performed the scatters were more pronounced on the curves with the electrode array oriented at right angles to the geoelectric strike of the intrusion. Ziji (1969) has noted that such scatters may be encountered when the dimensions of an anomalous body is too small and sounding curves are influenced by the resistant (or conductive) country rocks flanking the intrusion.

The field VES curves were visually smoothed, as suggested by Zohdy (1969), in order to be interpreted in terms of horizontally stratified laterally homogeneous media. The smoothed curves were given preliminary quantitative interpretation by method of curve matching, on the three-layer master curves published by Rijkswaterstaat (1975), and by determination of

the total longitudinal conductance of the geoelectric section from the right-hand positive gradient part of each sounding curve. The resistivities and thicknesses found in this way were used as starting values for further modelling with the aid of a computer programme which can calculate the apparent resistivity curve for any geoelectric section.

At two different sounding points, VESD and E (see fig. 4.3), cross electrical soundings were carried out. In cross electrical soundings, two soundings are carried out at a point in two mutually perpendicular directions. By this arrangements it could be possible to detect the dip of the intrusion and other causes of lateral effects such as folds and faults or contacts zones, the knowledge of which are necessary for accurate quantitative interpretations. Apart from greater distortions on the curves with the electrode arrays across the geoelectric strike in comparison with curves for electrodes oriented parallel to the strike, no recognizable evidence could be found in favour of substantial dip angle that may adversely affect interpretations based on horizontal layer models. The distortions in the curves have been attributed largely to lateral effects due to locations of the electrodes with respect to the boundaries between the intrusive body and the country rocks. Recall that lateral electrical discontinuities were observed across the boundaries during

the electrical profiling (see section 5.1.1).

Interpretations of H-type sounding curves are noted for ambiguity due to problems of equivalence and suppression. Within certain limits for which $h_2/\rho_2 = S_2$ remain the same, different sets of thicknesses and resistivities of the intermediate layer may produce the same sounding curve; these sets of parameters are said to be equivalent. Ambiguity due to suppression (or the principle of suppression) is related to layers with resistivities intermediate between the resistivities of the enclosing layers. Such layers if they are not thick enough, cannot be detected because they have practically no influence on the resistivity curves (Kunetz, 1966). The above suppression cannot be helped, but to check the limits of equivalence the values of h_2 and S_2 were adjusted by multiplying both of them by the same factor to obtain a new set of parameters which could best fit the field curves. The value of h_2 which produced the best fit has been considered as the best estimate of thickness of the intermediate layer for each sounding curve.

It was not possible to determine the transverse resistivities of the layers over the intrusive body. As a result it is not known whether the resistivity in the vertical direction is different from resistivity in the horizontal direction. In effect

anisotropy has not been taken care of in the following interpretations. The layers have been assumed to be horizontal and isotropic but not necessarily homogeneous.

TABLE 5.1: Resistivity Ranges for some Sediments, Rocks and Minerals (Telford et al 1976)

Rock Type	Resistivity range (ohm-m)
Unconsolidate Clay	20
Clays	1-100
Alluvium and Sands	10-800
Sandstones	$1-6.4\times10^{8}$
Granite	$3\times10^{2}-10^{6}$
Basalt	$10-1.3\times10^{7}$ (dry)
Gneiss (various)	6.8×10^{4} (wet)-3×10^{6} (dry)
Ilmenite	$10^{-3}-50$
Diamond	$10-10^{14}$
Natural water (igneous rocks	0.5-150
Natural water (sediments)	1-100

VES 8 at Yo 00 (Pit)

The sounding point was located at the pit at the intersection of two seismic spreads Yo Spread 2 and X_1 Spread 2 (fig. 4.3). The electrode array was oriented parallel to the geoelectric strike of the suspected kimberlite intrusion. The curve, as shown in fig. 5.10, is characterised by substantial scatter at the large spacings. Some of the scatters could be identified with changes in apparent resistivities due to changes in potential electrode spacing, for example, at $\frac{AB}{2}$ = 4, 7 15.8 and 31.6m. The rest have been attributed to lateral effects due to lateral inhomogeneities in subsurface layers.

The rising segment of the curve suggests a highly resistive substratum which resistivity has been estimated at 100 ohm-m but could be even higher. The conductive intermediate layer was found to be 8 to 17m thick with a resistivity range of 4 to 8 ohm. m. The equivalent property of this layer did not permit any unique solution but a thickness value of 10.1m and a corresponding resistivity of 6 ohm-m produced the best fit to the field curve. The low resistivity values suggest that this layer may contain clay with sandstone and also water. Incidentally grains of ilmenite were identified scattered around the pit; these may be a reflection of what obtains at greater depths in the ground.

The top alluvial soil has a resistivity of 200 ohm-m and was found to be about 0.9m thick. The highly resistive basement (1000 ohm-m) may contain sandstones, granite and basalt.

VES B at Yo 100 m SW

The rapid rise in the apparent resistivities coupled with the displacements, as revealed in the disconnected segments in the VES B (fig. 5.11) beyond $\frac{AB}{2}$ = 15.8 has made the reliable interpretation of VES B in terms of horizontally stratified and laterally homogeneous layers difficult. The displacements with increasing potential electrode spacing indicate the effect of strong lateral heterogeneities at depth, (Zohdy, 1969). The rapid rise in the apparent resistivity curves, in comparison with normal Schlumberger sounding curve for horizontal layers, shows that the array has probably crossed a buried vertical contact into a medium in which the underlying layer is more resistant, that is, the kimberlite-host rock interface.

Nevertheless an interpretation was attempted as done for VES A. The resistivity of the top soil layer is in the range of 90-100 ohm-m and has a mean thickness of about 3m. The second layer was found to have a mean resistivity of 40 ohm-m with a thickness range between 7 to 13 m. The resistivity of the basement rock was again taken at 1000 ohm-m.

VES D at X_1 60 m NW

The centre of the array was located on a seismic station so that the results of the sounding could be compared with and checked against the seismic refraction results. Cross soundings were performed at this station in order to determine the best orientation for the Schlumberger array and also to determine if possible the dip of the layer. Both soundings produced about the same results, the curves having considerable scatter at large spacings, f g. 5.13 D_1 and D_2. At short electrode spacing the curve D_1 for the array parallel to the geoelectric strike (of the intrusion) is smoother. The sharp discontinuity in D_1 beyong $\frac{AB}{2}$ = 40 indicates the presence of some strong lateral inhomogeneities. The upward displacement suggests that one of the potential electrodes has probably crossed over into a medium of higher resistivity. The slope of the rising segment of the curve may offer additional indication to support the above interpretation. Kunetz (1966) has suggested that when a current electrode crosses a contact or interface between two adjacent formations of different resistivities, a discontinuity in the rising segment of the sounding curve such as has been observed in fig. 5.13 (D_1) may be encountered, and particularly, if the centre of the array is down thrown from the

contact and the underlying bed has a lower resistivity the fall in the sounding curve observed in D_1 (fig. 5.13) between $\frac{AB}{2}$ = 15.8 and 40m may be expected.

In view of the fact that accurate geologic controls/drill hole data are lacking for this station, and actually for the whole survey area at large, accurate quantitative interpretation of the curves (D_1 and D_2) was not possible. However, by visual smoothening of the curves attempt was made to estimate the geoelectric parameters. The surface layer was found to be 1.5 thick with resistivity of about 12 ohm-m. From table 5.1 it appears to be alluvium mixed with sand. The intermediate layer may be clay, with resistivity of 8 ohm-m and an uncertainty of 10%. The thickness of the clay layer was estimated at about 3 m. The apparent resistivity of the bottom resistive layer was about 120 ohm-m, and this falls in the resistivity range for (wet) igneous rocks (table 5.1).

VES E at X_2 45 m NW

Cross soundings were carried out at this station and the results are given in fig. 5.14. E_2 was oriented at right angles to the strike and therefore cut the vertical contacts of the diatreme-hostrock transition resulting in highly scattered, uninterpretable data.

The characteristic features of E_1 are similar with features observed for sounding curves at other stations. Again the final segment (with positive slope) was found to have substantial fluctuation. The discontinuities suggest near-surface inhomogenecities rather than lateral variations in resistivities at depth.

The resistive surface layer (380 ohm-m) was found to be about 2.1 m thick. It is the dry top alluvial/sandy soil. The intermediate layer containing clay/sand or sandstond has a mean thickness of 23 m, and an apparent resistivity in the range of 11-12.5 ohm-m. This low apparent resistivity value suggest the bed may contain water and probably ilmenite as well (see table 5.1). The bottom layer was found to have a resistivity of about 1000 ohm-m.

VES E_2 AT X_3 30 m NW

The measurements at this station were made with the array layed in a direction parallel to the geoelectric strike of the intrusion and the results are shown in fig. 5.15. The conductive intermediate layer has a mean thickness of about 10.2 m and resistivity of 3 ohm-m. The low resistivity indicates that the bed may contain much water as well as clay and sandstone.

The asymptote method of interpretation used on the rising portion of the curve suggests that the resistive basement may be at a depth between 9 and 12 m. The resistivity of the basement has been estimated at around 1500 ohm - m, a value typical of hard rocks like granite and basalts. The thickness of the dry top soil layer has been estimated at 1 m, with a resistivity of 200 ohm-m.

VES H at Yo 380 m SW

Fig. 5.17 shows the data for VES H. The resistivity of the basement has been estimated at about 3000. Asymptote method of interpretation used on the rising segment of the curve suggest the basement is located at a depth of 10 to 18 m under the ground surface. The intermediate conductive layer has a mean thickness of about 15 m with a resistivity range of 8 to 10 ohm-m. Its equivalence property made it difficult to determine the unique parameters for this bed. The resistivity range suggests the intermediate layer may contain sandstone, clay, water.

Two seismic refraction spreads (one along the baseline Yo and the other on traverse X_5) covered this resistivity sounding station.

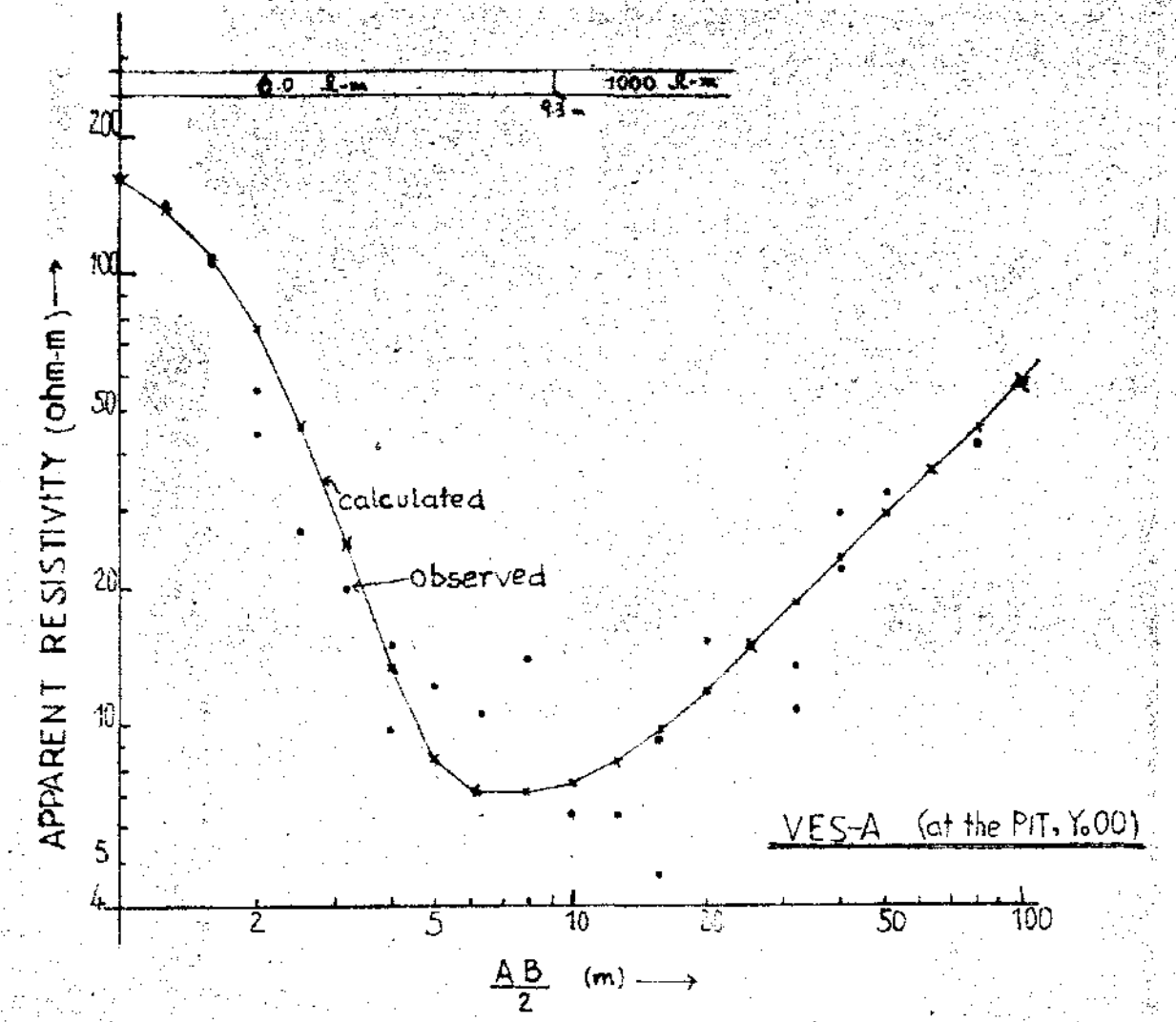


FIG. 5.10 Three layer interpretation of VES A

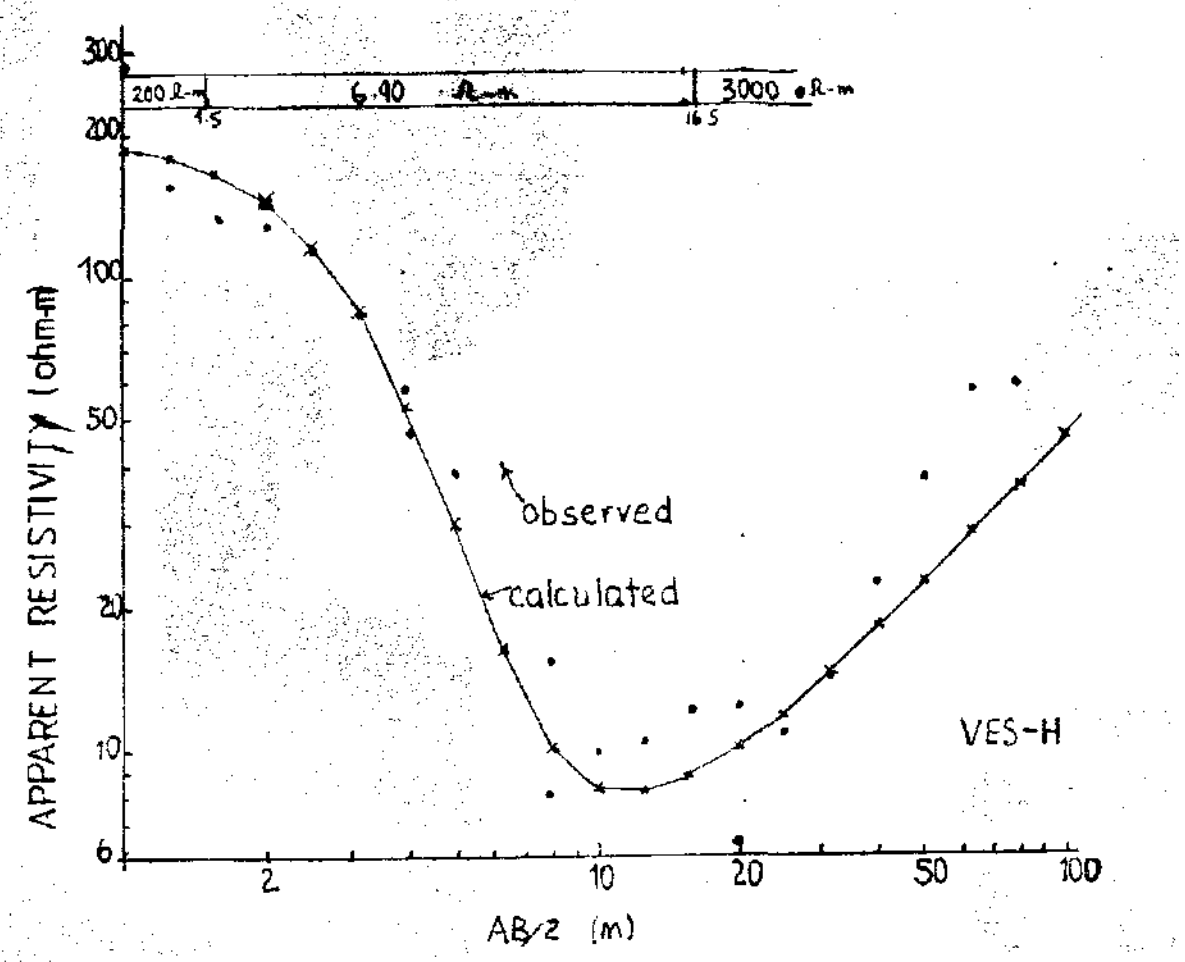


FIG. 5.17 Three layer interpretation of VES-H

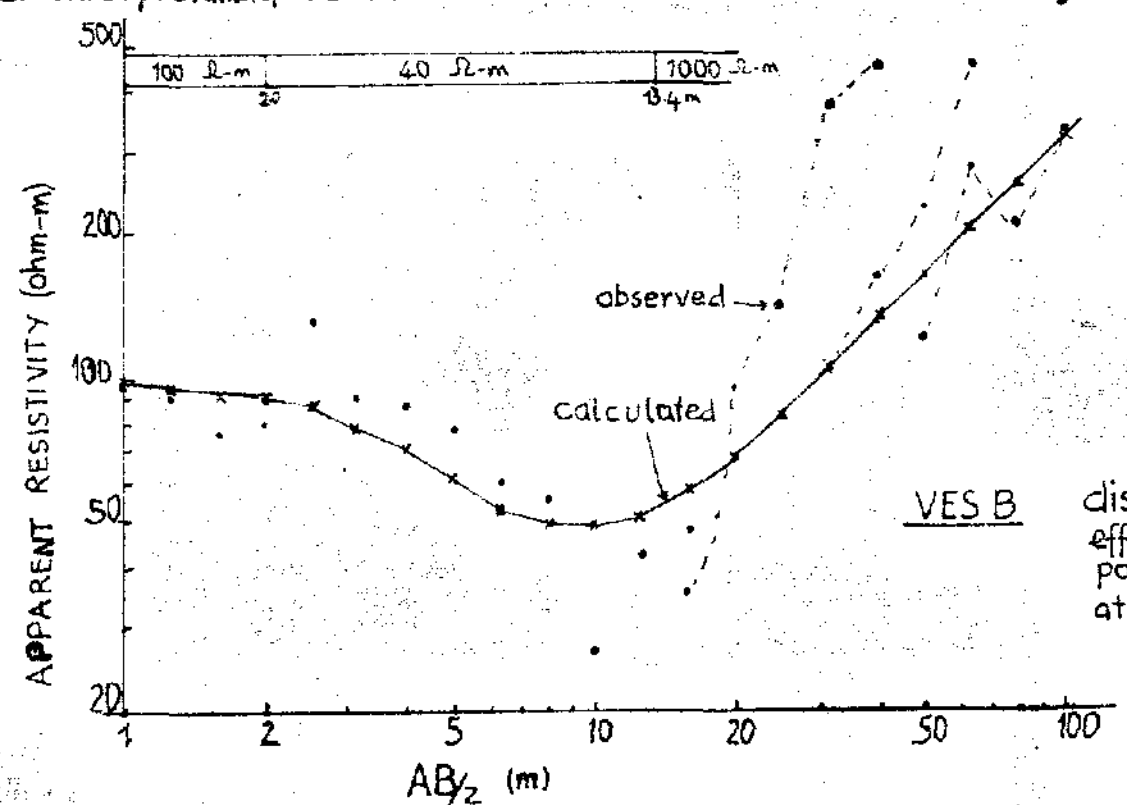


FIG. 5.11 Three layer interpretation of VES B

VES B disconnected segments show effect of change of positions of potential electrode on VES curve at large spacing (AB/2)

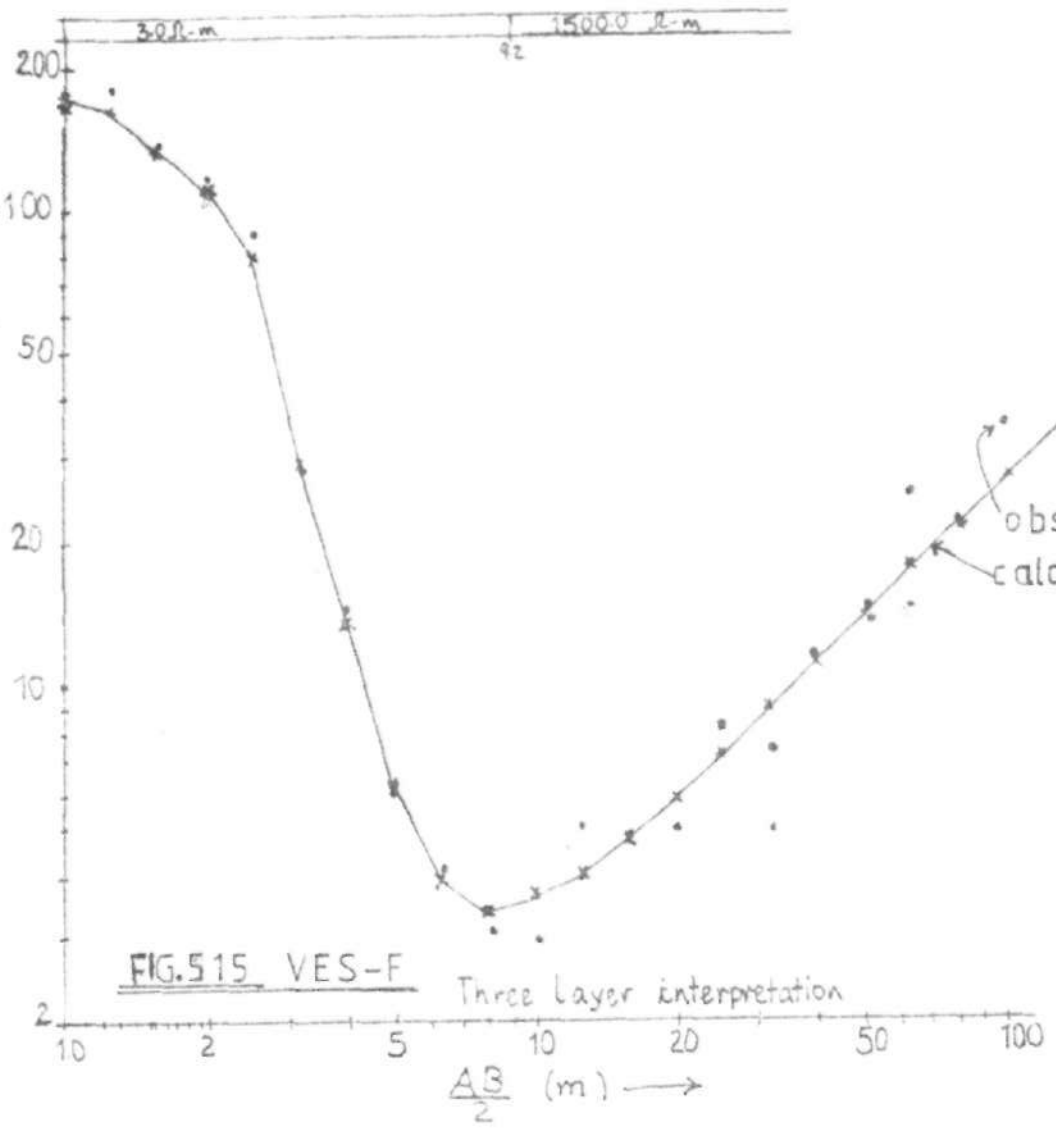
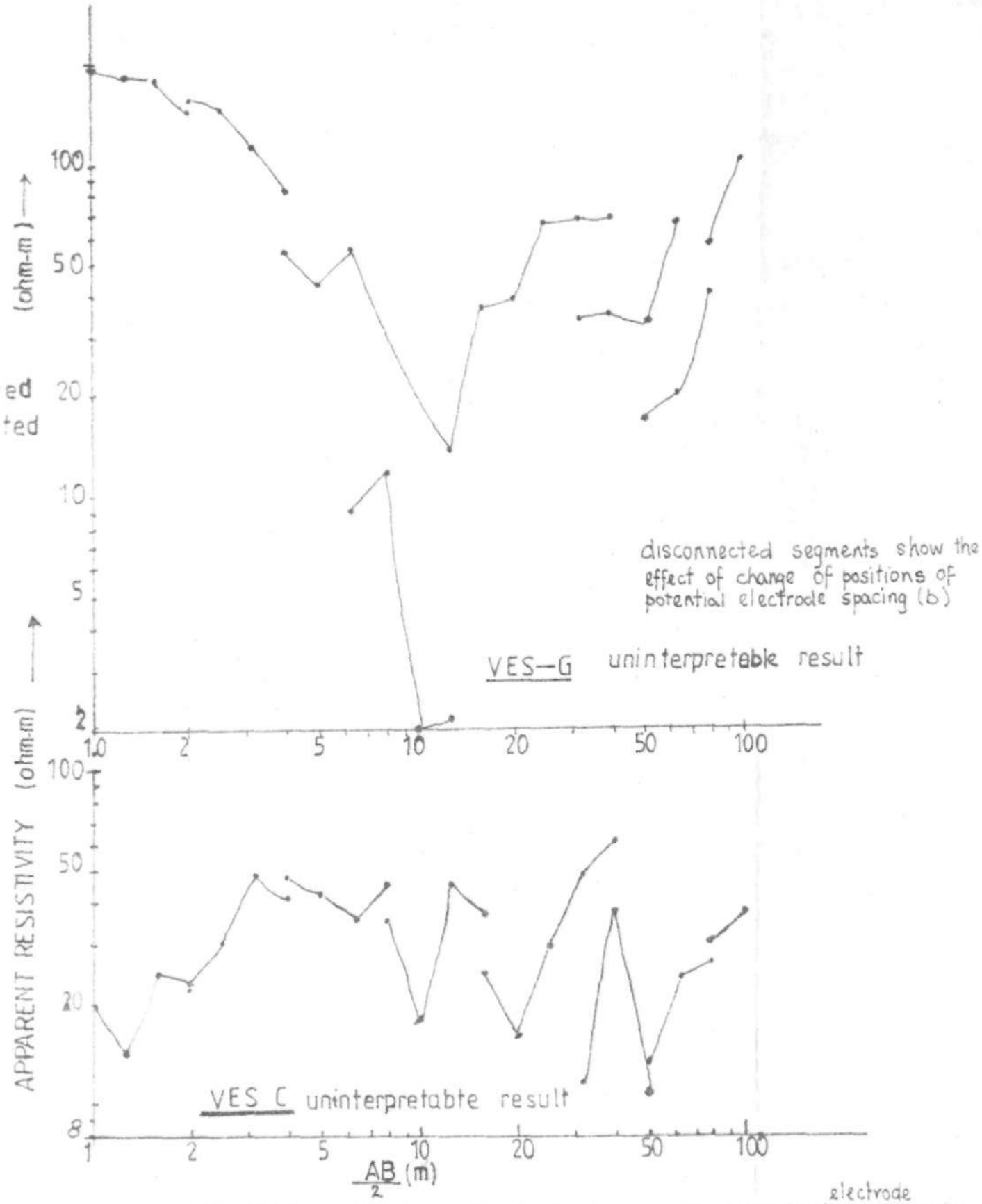


FIG.515 VES-F Three layer interpretation



disconnected segments show the effect of change of positions of potential electrode spacing (b)

VES—G uninterpretable result

FIG. 5.16 showing effect of change of potential electrode spacing (b) VES curves

VES C at X_4 0 (or Va 300 mSW) and
VES G at X_4 15 m NW

The results of VES C and VES G were as given in fig. 5.12 and fig. 5.16, respectively. The data are quite scattered and no interpretation could be done. In view of the narrow width of the pipe on traverse X_4 (fig. 5.6) and also the lateral variations in its width along the strike (figs. 5.8 and 5.9) the irregular behaviour in the sounding curves is expected. At these stations the lateral inhomogeneities have shown up as electrodes effects near the potential electrodes as can be observed in the disconnected segments of the sounding curves. Each of the segments in the two curves corresponds to different potential electrode seperation.

Summary of Resistivity Sounding Results

In the group of the interpretable results the VES curves obtained were the H-types, in which the resistivity of the surface layer was found to range between 12 and 400 ohm-m with a mean value of 210 ohm-m. The thickness of the layer varies from 0.9 to 3.2 m with a mean value of about 1.5 m. The conductive intermediate layer has a resistivity ranging from 2 to 40 ohm-m, with an average value of 12 ohm-m. The low resistivities of the intermediate layer suggest presence of clay with sandstones.

The mean thickness of the layer is 13 m. The resistive basement has a resistivity range of 122 to 3000 ohm-m with estimated average of over 1000 ohm-m. Because of the absence of drill holes data and reliable geological controls the intrinsic parameters of the geoelectric sections were not available for checking the accuracy of the VES results. A maximum error of 16% is expected in the apparent resistivity measurements on the basis of..... The summary of the results for individual sounding points is given in Table 5.2.

Fig. 5.12 gives a picture of the variations in the apparent resistivities and geological formations with depth for the near surface layers of the Kafur/Massari kimberlite pipe. The resistivity sounding points (VES's D to H) were situated on a profile DH on the geoelectric strike of the intrusion (see fig. 4.3). The geological interpretations were obtained by comparing the apparent resistivities determined from the sounding curves at indicated VES points with those in Table 5.1. It has been assumed in producing this picture that the geoelectric sections and hence geological formations are continuous between the VES points. At G, the sound curve could not be interpreted and the dashed lines have been used to indicate some uncertainty in the picture at this sounding point.

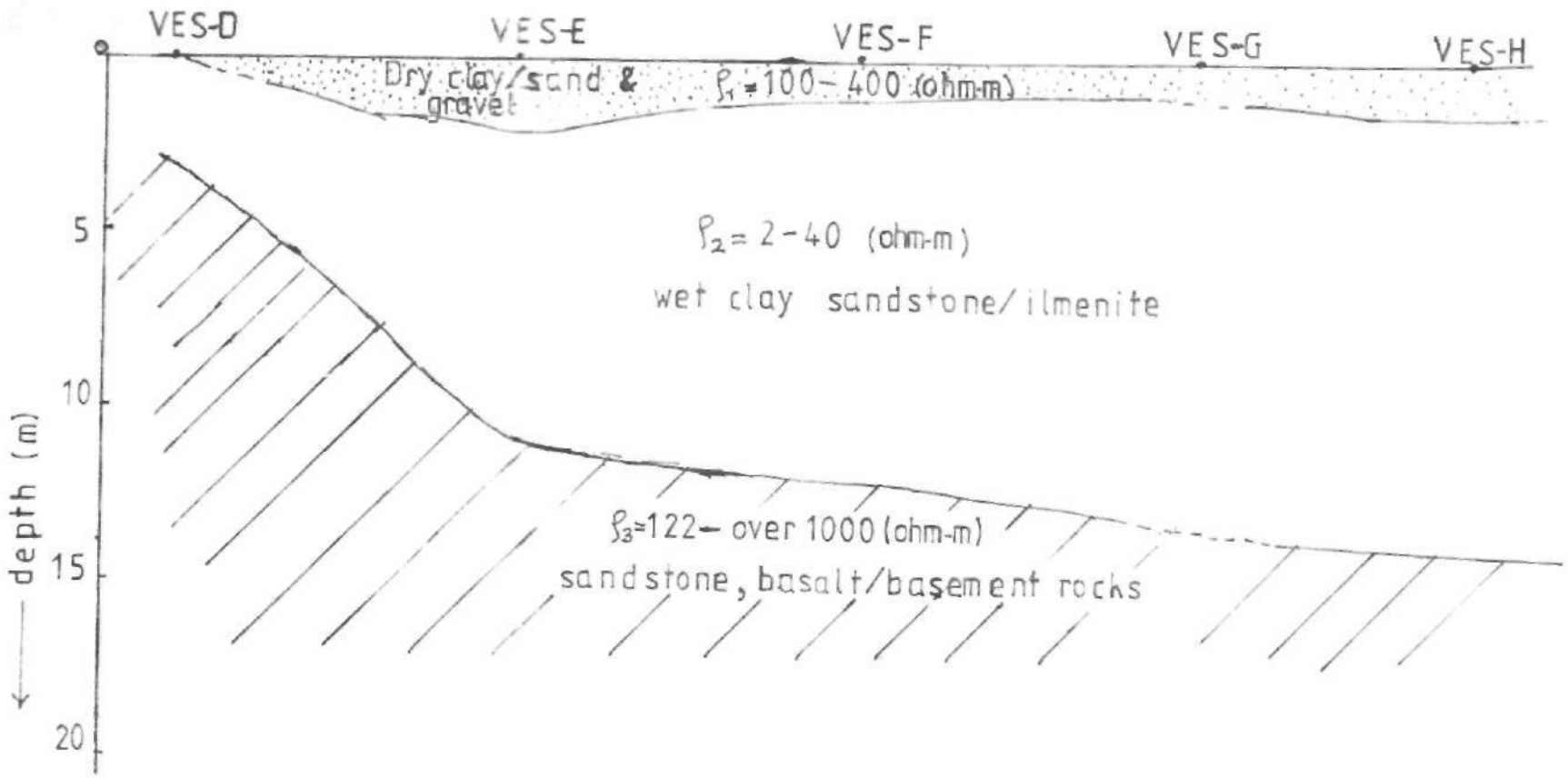


FIG 5.17 The geoelectric sections and the corresponding geological interpretations for a VES profile DH on the kimberlite pipe

TABLE 5.2: Summary of the results of VES measurements at each sounding point.

VES Points	Resistivities of layers (phm-m) ρ				Thicknesses of layers (m) h_2 (m)			
	1	best fit	equivalent range	3	h_1	best fit	equivalent range	h_3
A	200.0	6.0	4.0-8.0	100	0.9	10	7.5-17.1	-
B	100.0	400.0	-	1000	3	11.2	7-13	-
C -	N O T I N T E R P R E T E D				-	-	-	-
D	12.5	8.13	-	122	1.0	3.0	-	-
E	384.0	11.5	10-14.0	1000	2.1	22.9	17.9-26.0	-
F	200.0	3.0	2.0-4.0	1500	1.0	10.2	9-12.0	-
G -	N O T I N T E R P R E T E D				-	-	-	-
H	200	6.9	5.4-8.4	3000.0	1.5	15	8.5-16.5	

5.2 INTERPRETATION OF SEISMIC REFRACTION DATA

Interpretation Methods - A Brief Review: In the interpretation of the seismic refraction data, the reciprocal method of routine shallow seismic refraction investigations, as detailed by Hawkins (1961), was used to determine the depths to the refractors in details.

The method is based on a term called "time-depth." Hawkins described the "time-depth" to a refractor as the time delay associated with the critical ray in travelling between the refractor and the surface. It will be pointed out that "Time-depth and "half-intercept time" are not exactly the same. Time-depths can be isolated at all geophone stations but half-intercept times can be determined only at the shotpoints. With time-depths it is possible to determine the depth to any particular refractor at all geophone stations as well as shotpoints in order to produce a detailed profile of even an irregular refractor. On the other hand, with half-intercept times (where the refractor is assumed to be plane between shotpoints) depths are obtained only at the shotpoints. Hawkins Reciprocal Method differ from the Delay-time method of Gardner (1939) and Nettleton (1940) in that the latter assumes the refractor is horizontal below the geophone station while the former assumes plane refractor surface (which

is not necessarily horizontal) at the geophone station.

The time-depth at a geophone station is obtained by the procedure illustrated in fig. 5.19.

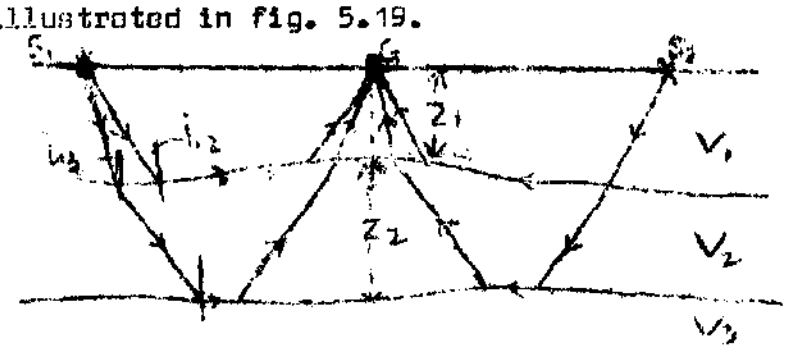


Fig. 5.19: Ray paths of critically refracted rays used in determing time-depth to refractor.

The time-depth is $tG = \frac{1}{2}\ t\ (S_1G) + t(S_2G) - t(S_1S_2)$

where $t(S_1G)$ and $t(S_2G)$ are the travel times of the refracted rays between the receiving point G and the colinear shotpoints located on opposite sides of G. $t(S_1S_2)$ is the travel time between shotpoints known as reciprocal time.

Writing t_1 for the time-depth the thickness of the first layer below G is obtained by using the relation.

$$Z_1 = t_1\ V_1/\cos i_{12}$$

and thickness of the second layer by using

$$Z_2 = \left[t_2 - Z_1\ \frac{\cos i_{13}}{V_1}\right]\ V_2/\cos i_{23}$$

In the general form the thickness of the nth layer Zn is

$$Zn = \left[tn - \sum_{K=1}^{n-1} Zk \frac{\text{CoSiK, n+1}}{Vk}\right] \frac{Vn}{\text{CoSin, n+1}}$$

[1]The half-intercept time and delay time may be used to replace the time-depth (tn) at shotpoints.

The velocity of the refractor (in this survey) was determined by using the "Plus-Minus" method of Hagedoorn (1959). In Hagedoorns method the difference between two critically refracted rays from shotpoints S_1 and S_2 to the geophone G (fig. 5.19) is determined. The result is called the "Minus" value for the refractor at that geophone G. The Minus values at other geophones enclosed by the two shotpoints S_1 and S_2 are determined and plotted against the horizontal distance. The slope of the minus graph gives the true velocity of the refractor. Hagedoorn has pointed out that the 'Minus' graphs yield much more accurate velocity values than the graphs of travel time against distance, because any affects (such as variations in velocity and thickness) of the weathering (surface) layer on the refractor velocity are eliminated by the process of subtracting pairs of travel times from the same refractor to each geophone. Hawkins (1969) commended the accuracy of the Plus-Minus method.

These detailed analytic methods - the Reciprocal method and the Plus-Minus method - were considered necessary in order to be able to interprete the seismic refraction data more accurately as dependable geologic controls or drill holes data are lacking for the survey area.

5.2.1 Refraction Survey on Yo

On the Yo traverse, 5 spreads were shot by the continuous profiling method. The travel time curves were plotted and the apparent velocities determined as in fig. 5.21.

(a) Yo Spread 1-3: The three spreads extended from 100 m NE to station 170 m SW. (Only spreads 2 and 3 are shown in fig. 5.20). They were interpreted together because of some similarities in the travel time curves. Spreads 1 and 2 were made to overlap 7 geophone stations for thorough investigations of the discontinuities in the curves between station 10 and 20 m NE. They suggest the presence of a buried interface with vertical contacts between two rock types of different seismic velocities located between 10-20 m NE (see also fig. 5.21). The displacements in the curves indicate rapid change in the thickness of top soil layer across the discontinuity. The travel time curves from the end shot points (at 55 m NE and 65 m SW)

TABLE 5.3.1: Representative velocity values (Mooney, 1977)

Material	Velocity Range (m/s)
Weathered surface material	300 - 600 (300 - 900
Gravel or Sand (dry)	450 - 900
Sand (wet)	600 - 1800
Clay	900 - 3000
Sandstone	1830 - 3970
Granite	4580 - 5800
Metamorphic rocks	3050 - 7020
Gneiss	3500 - 7500
Sand (Loose)	200 - 2000
Basalt	5060 - 6400

represent two layer subsurface structures. The apparent velocities on the longshot curves suggest that a deeper higher velocity analysis shows that to the left of the buried interface there exists a shallow high velocity material of mean seismic velocity of 4850 m/s underlying an overburden of variable thickness and velocity. The variations in the surface layer velocity may be attributed to local inhomogeneities in the layer. To the right of the buried interface the situation is different. The interpreted velocities suggest two different refractors below the surface layer; one with a velocity of about 2460 m/s and the other 3260 m/s. Depth analysis indicated that the 3260 m/s refractor probably sandstone/metamorphic rock formation (Table 5.3) is at an average depth of 40 m. The intermediate layer (V_2 = 2460 m/s) probably the weathered bedrock containining clay with sand/sandstone is about 26-32 m thick. The velocity of the shallow bedrock to the left of the interface falls in the velocity ranges for granitic/metamorphic rocks. It was observed that granite basement rocks outcrop in that region.

The results of spread 3 show another buried interface located between 110 and 120 m SW. The travel time curves suggest a one layer model. To the left of the interface the second layer

has a mean velocity of about 2420 m/s which compare well with the velocity of the second layer in spread 2. These layers may be the extension of each other. To the right of the second layer is a high velocity formation. The formation has a mean velocity of about 4000 m/s which indicate the presence of metamorphic rock or basement gneiss. Across the contacts the formations on both sides are probably at different depths. This may account for the fall in the first arrivals in the curves between stations 110 and 130 m SW. The similarities in the spreads may be seen in the velocities of the formations on both sides of the buried interfaces and the fact that the higher velocity formations are shallower than the (weathered) formation between them.

(b) Yo Spread 4: The spread extended from 170 to 280 m SW on traverse Yo. For this spread a single layer model of interpretation is suggested with a buried vertical interface to be located below station Yo 224 m SW.

To the left of the interface the velocity of the refractor range from 3630 to 4070 m/s while to the right of the interface the refractor has a velocity of 2500-3300 m/s. These velocity ranges suggest that the rock type to the left may be the extension of the metamorphic/basement gneiss rocks suggested in

spread 3 (fig. 5.20), and the rocks to the right of the interface may be identified with the clay and sand/sandstones layer encountered also in spread 2 and 3 in the last section.

The velocity, 520 m/s, for the surface layer was determined from the results from the endshot situated at station Yo 285 m SW alone. This was because the results from other shots in the spread did not produce accurate enough data on the surface layer. It is understood (and should be noted) that the thickness of the surface below each station is subject to the accuracy of the surface layer velocity, here and elsewhere.

(c) Yo Spreads 5: This spread overlap spread 4 at station 280 m SW and extended to 390 m SW (fig. 5.21). The endshot results suggest a three layer model of interpretation and the velocity of the third layer was found to be about 2440 m/s.

But a velocity of 3260 m/s obtained from the longshot arrivals indicates fourth refractor.

Layer one has a variable velocity, about 400-560 m/s and a maximum thickness of 5 m. The velocity suggests a sandy soil material. The second layer may contain (wet) sand/clay with velocity of about 1280 m/s. The velocities of layer 3 and layer 4 were found to be 2440 and 3260 m/s respectively. The third layer has an average thickness of about 30 m. The

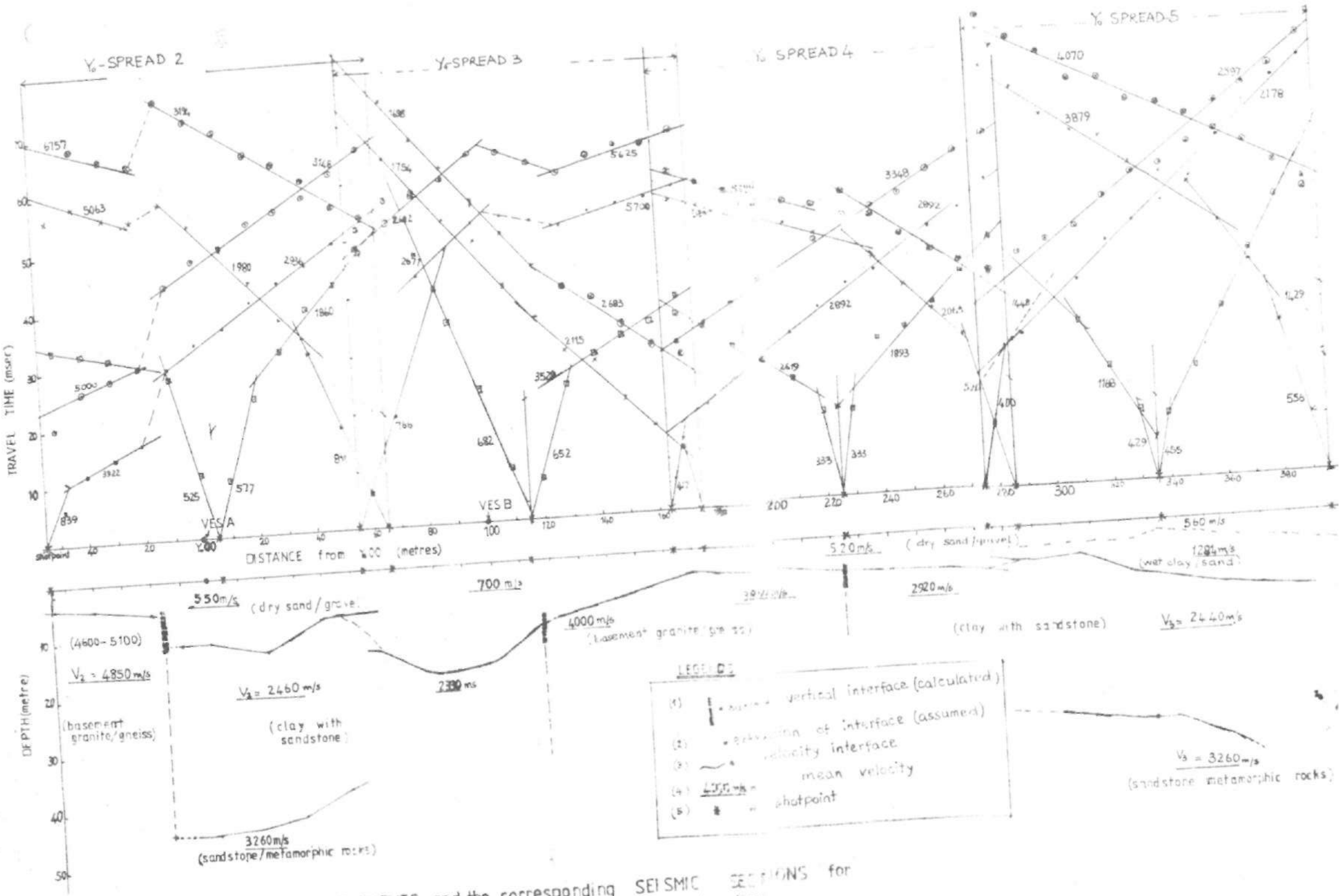


FIG. 5.21 TRAVEL TIME CURVES and the corresponding SEISMIC SECTIONS for REFRACTION MEASUREMENTS on TRAVERSE Yo-the baseline

velocity suggests that it probably contain clay/sandstone. Layer 4 is found at 36 to 43 m below ground surface. The velocity again suggests sandstone/metamorphic rock types or weathered bedrock. The velocities of layers 3 and 4 correlate well with the velocities obtained for layer 2 and 3 in Yo spreads 2 and 4 (fig. 5.21).

In this interpretation a hidden second layer has been suspected below the shotpoint at 275 m SW. The second layer is thought to be either too thin to produce refracted arrivals at the surface or it may be absent below the station. The substantial scatters in the curves may be attributed to undulation at the refractor surfaces or some local changes in composition of the formations.

5.2.2 Refraction Survey on X_1

In fig. 5.22 are shown the combined travel time curves and the corresponding interpreted sections for the three spreads shot on this traverse. The individual spreads are as indicated.

Analysis and comparisons of the travel time curves show that spread 1 crossed a buried vertical interface near X_1 140 m NW, spread 3 crossed a similar interface near X_1 20 m SE while spread 2 is right on the top of the pipe. The seismic velocities on the opposite sides of the above interfaces compare well with

those associated with similar interfaces found in spreads 2 and 3 on traverse Yo (fig. 5.22).

In fig. 5.23, the high velocity refractor with seismic velocity in the range of 4800-5000 m/s (spread 1) and 3850-5000 m/s (spread 3) is the basement granite/gneiss which form part of the country rock that flank the pipe. Over the three spreads on traverse X_1 the velocity of the surface layer vary between 500 m/s to 870 m/s. The surface layer velocity (500 m/s) used in spread 1 was actually obtained from the data of spread 2 basically because in spread 1 there is no adequate data on the surface layer and it is assumed that the velocity does not change very much over the two spreads. The thickness of this layer vary between about 3 to 10 m.

In spread 2, over the pipe, the second layer has a velocity which vary from 2200 to 2760 m/s. A third layer with velocity of 3450 m/s was also detected. The second layer may contain clay mixed with sandstone, it is 10-30 m thick. The third layer is probably weathered bedrock.

Spread 3 crossed a basement outcrop between location 80 m stand 90 m SE on X_1. The fall in the travel times to the right of these stations may be attributed to a shallow basement rock which might have outcropped there.

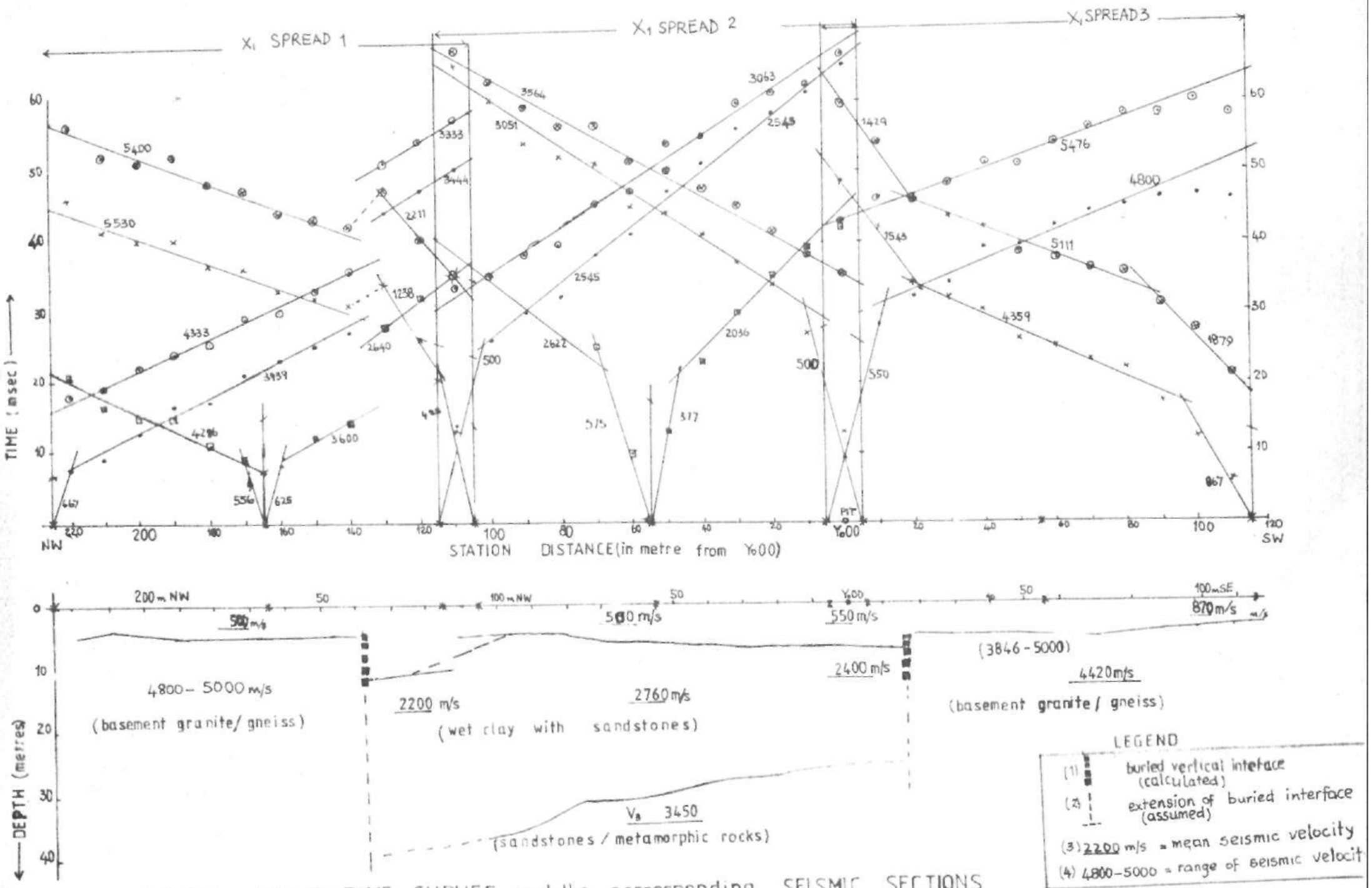


FIG 5.22 TRAVEL-TIME CURVES and the corresponding SEISMIC SECTIONS for REFRACTION MEASUREMENTS on TRAVERSE X_1 (GEOLOGICAL INTERPRETION BASED ON SEISMIC RESULTS AND GENERAL GEOLOGY OF THE AREA)

Refraction Survey on Traverse X_5

One spread was shot on this traverse and the travel time curves were as in fig. 5.24.

A close study of the curves shows evidence of lateral inhomogeneities in the subsurface layers. In the second layer, for example, a vertical velocity interface may be located near station 5 m SW - particularly on the basis of the closeness of the points of change of slopes on the curves for shotpoints located east of the X_5 0 (Hawkins, 1961). To the left of the interface V_2 = 2670 m/s was found while to the right V_2 = 1450 m/s was obtained. The velocity of 1450 m/s suggests that water may be found to the right of the interface.

The seismic results are ambigous concerning the parameters of deeper layers. The behaviour of the third segments of the curves for shots fired from the NW of the spread is not clear The fall in the values of the first arrivals between station 20 and 30 m SE indicate velocity increase which may be caused by change (decrease) in the depth of layer two or arrivals from deeper refractor.

The velocity of the surface layer range between about 385 and 670 m/s, but the average value, 530 m/s, was used in depth estimations. The maximum thickness of this layer obtained was about 6 m.

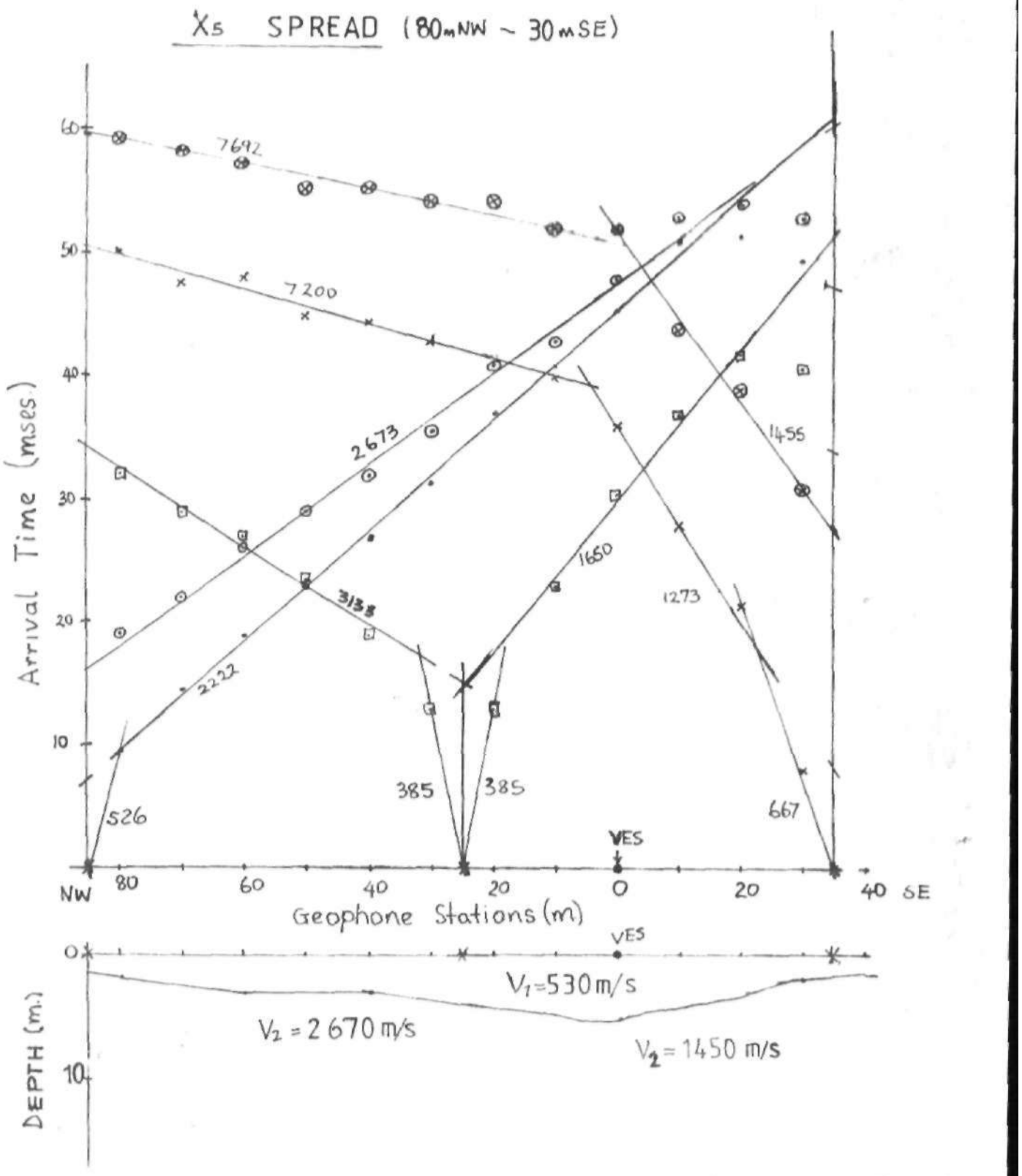


FIG. 5·23 TRAVEL TIME CURVES & SEISMIC SECTIONS
REFRACTION MEASUREMENT on TRAVERSE X5

Summary of Seismic Refraction Results

Two different velocity zones separated by buried vertical interfaces were revealed by the seismic refraction results. The two zones were found to be overlain by a top soil layer of variable thickness whose velocity range between 500 to about 870 m/s. One of the two zones was found to be enclosed by the interfaces while the other lie on the outside of the interfaces. The zone on the outside was found to be a shallow high velocity bedrock (with true velocity between 4000 and 5100 m/s) immediately underlying the thin surface layer, about 4 m thick. The high velocity has been interpreted to represent basement rocks including granite/gneiss and or metamorphic rocks.

Enclosed by the buried interfaces a (dyke like) vertical structure was found. At the top of this structure the surface layer was relatively thicker (6-15 m) than over the high velocity zone mentioned above. Below the surface layer was a layer with a velocity range between 2000 and about 2760 m/s, indicating the presence of clay with sand and sandstones. The thickness of this bed was found to vary between 17 and 34 m. The top surface of a deeper layer of sandstone/metamorphic or weathered bedrock with velocity between 3260 and 3450 was mapped with the seismic refraction method. The results of the interpreted seismic

data were as given in the composite seismic sections and the corresponding travel time curves in fig. 5.21 and fig. 5.23 for the seismic refraction spreads on traverses Y_0, X_1 and X_5.

A close look at the travel time curves in fig. 5.21 and fig. 5.22 will reveal that the endshot and centre shot results did not produce adequate data on the surface layer velocity. The variations in the velocity are therefore not known, in particular, the velocities (of the surface layer) could not be determined as the author thought it objectionable to fit lines through single observation points (for shotpoints situated at stations Yo 55 m NE and Yo 165, 175 m SW in fig. 5.21, for example). To determine the thicknesses of the surface layer a mean velocity for the medium was deduced from the slopes of the appropriate segments of the endshot and centre shot travel time curves, where it was found reasonable to fit line through the data points. Such mean velocity for each spread was used to calculate the thickness of the layer below the geophone stations.

In the seismic sections the thick (broken) vertical lines (e.g. at Yo 15 m NE and Yo 117 m SW, fig. 5.21) indicate the regions where the contacts may most likely be located. The thin (broken) vertical lines extending downwards from the thick ones only suggest the probable continuation of the contacts with increasing depth.

C H A P T E R VI

DISCUSSION

6.1 THE RESULTS

(a) Resistivity Profiling: Using constant electrode spacings (Wenner array) located the pipe and established the boundary between the pipe and the surrounding. No definite geometric pattern could be associated with the pipe although it was found to be elongated in one direction. Its width was found to vary along the preferred direction (east of NE) - see figs. 5.8 and 5.9. Vertical electrical soundings (VES) using Schlumberger arrays identified the H-type resistivity layer models on top of the pipe except at two stations where the VES curves could not be interpreted. Where they could be interpreted, heterogeneous conditions in the electrical properties of the near-surface layer which gave rise to displacements on the curves and lateral variations in the resistivity at depth which resulted in sharp discontinuities on the curves at large electrode spacings throw doubts on the reliability of the interpreted geoelectric parameters of the third layer. In addition,

due to equivalence property and lack of borehole data, the accuracy of the Schlumberger sounding method is rather low in the determination of the thickness of the second layer.

The seismic refraction method was successful in locating the contact between the pipe and the surrounding country rocks but not as obvious as the resistivity method. The layer structure on the top of the pipe was however much better determined with this method. Over the country rock a two layer model was obtained. The velocity of the surface layer varies between 430 and 870 m/s while the velocity of 3840-5100 m/s was obtained for the refractor. The high velocity contrast indicates that an hidden intermediate layer (if present) was not detected by the seismic refraction method because the layer was either too thin or absent over the country rock. The first arrival breaks were quite clear but the second arrivals were hard to pick in most cases. As a result nothing could be done to resolve the problem. On the other hand over the kimberlite intrusion three layer models were obtained. The surface layer was observed to be thicker over the top of intrusion than over the country rock. The summary of the results has been given in fig. 5.21 and fig. 5.23.

(b) Correlation between Refraction Results, Resistivity Anomaly and Local Geology: Correlation of seismic velocities of shallow structure with resistivity profiling results has shown close agreement between the regions of anomalous (low) apparent resistivities with region of low seismic velocities. The resistivity result established that the region of low resistivities correspond with the location of the pipe. There is general agreement between the seismic sections and the electrical sections from the VES results (although their respective values for the thickness of the surface layer are different). Almost identical geological formations were deduced for the corresponding layers obtained from the VES and refraction results. On traverse Yo where VES C results were found to be ambiguous refraction results suggested four-layer model. The failure of the sounding method to clearly distinguish between the resistivity layers may be attributed to the effect of the problem of suppression.

With regards to the local geology of the area, the surface plan and orientation of the intrusive pipe as deduced from the results of the present survey compare favourably wth the information reported by Wright (1976) - see section 3.1. It has been found from this survey that the pipe is 560 - 660 m long

and about 140 m wide at widest point. This survey also confirmed that the pipe is orientated in direction east of NE.

The results of this survey compare well with the results of the work of Verheijen and Ajakaiya (1979) but not in the magnitudes of all the physical parameters. For example, the resistivity of the dry top soil layer was found to be 700 ohm-m by them, as against an average value of 210 ohm-m (obtained from resistivity of 12-400 ohm-m) during this survey. Also their gravity model does not correlate with the seismic models obtained in this survey. Their model assumed a uniform density for a pipe which probably outcrop at the surface. The author feels that for an intrusive pipe which is weathered at "shallow" depth (a fact they accepted) the gravity model should reflect the fact that density contrasts decrease with depth and that the pipe is not observable at the surface. This is not to say that both the gravity and magnetic field anomalies are not accepted by the author.

(c) Existence of Kimberlite and Ground Water: The integrated results of all the geophysical surveys are consistent with geophysical results obtained over typical kimberlite pipe in other parts of the world as reported by Gerryts (1967) and Paterson et al (1977). It was pointed out (chapter 3) that where geology

methods failed, geophysical methods have proved successful in locating kimberlites.

According to McCurry the Diamond Company of Sierra Leone which located the pipe abandoned it. As a result, Turner (1975) speculated that the pipe does not contain kimberlite. The author does not share the opinion of Turner for the reasons that his only two pits at 80 m apart were shallow (5 m deep) and probably did not sample deep enough into the pipe. It may also be argued that the Diamond Company which was searching for the source of several diamonds found in Northern Nigeria (McCurry, 1970) probably abandoned the pipe not because it was not a kimberlite pipe but may be diamonds (of commercial quantity) was not found in the pipe. Recall that it was pointed out in Chapter I that not all kimberlite (pipes) contain diamonds.

As regards the location of groundwater reservoir the low apparent resistivities about 13 ohm-m (average) suggest that much water may be contained in the pipe. It is likely that a dug well situated anywhere within the outline of the pipe will be a source of ground water supply, but the seismic results (on X_5 spread) indicated the water table is closer to the surface at around station Ys 380 m SW.

(d) Structural Trend-lines and Kimberlite Emplacement:-

The major NE - SW transcurrent fault mapped by McCurry (see fig. 2.2) and the Maseri/Kafur Kimberlite pipe have nearly parallel orientation. The implication is that the transcurrent fault may not be unconnected with the emplacement of the Maseri/ Kafur Kimberlite pipe. It may be postulated that during the metasediment belt by upto 10 km McCurry, (1970) some cracks and or fractures might have been generated in the crustal material (basement rock) over some deep-seated tension fractures at the site of the Kafur kimberlite pipe. Such cracks or fracture zones constitute sub-surface zones of weakness favourable for the intrusion of upper mantle material; thus the Kafur kimberlite pipe.

It has been found that kimberlite pipes normally occur in groups of at least two (Dawson, 1967). That being the case, the Kafur pipe may not be the only kimberlite pipe in the area. The intersections of the major transcurrent fault for example, with the displaced metasediment may be worth detail investigation with both geological and geophysical methods to find what possible anomalies may be associated with them. Kimberlite intrusions have been located (e.g. in the U.S.A.) at the intersection of faults with zones of parallel structure. Such intersections

are points of excessively weakened crust and probable localities for the intrusion of upper mantle material (Parish, 1978).

Also the structural trend-lines in fig. 2.2 may be surface manifestimation of some lineations in rocks at depth. They may mark zones of structural discontinuity, intense shearing as well as zones of mineralization. Such trend-lines may show up as gravity/magnetic lineations. Extensive gravity and magnetic field survey could then help to define the lineaments. Buried intrusions may exist at the junctions of the lineaments.

6.2 CONCLUSION

In conclusion it may be said that:

(a) Resistivity method has re-located and delineated the Kafur/Kaseri Kimberlite pipe.

(b) The pipe is oriented in a direction east of NE. At its surface it is about 560 - 660 m long with a maximum width of 140 m.

(c) The pipe is covered by sandy soil and gravel material about 6 to 15 m thick. The seismic velocity of this surface material varies from about 500 to 870 m/s and the mean apparent resistivity is 210 ohm-m.

(d) A layer (17-34 m) thick with seismic velocity ranging between 2000 and 2760 m/s and mean apparent resistivity of about 13 ohm-m forms the top ortion of the pipe. This layer may be the decomposed and oxidized kimberlite - the "yellow ground," containing clay minerals, water and sandstones.

(e) A deeper layer of "weathered" bedrock with seismic velocity about 3360 m/s and apparent resistivity increasing with depth from 122 to over 1000 ohm-m was detected an the pipe.

(f) The country rock is basement granite/gneiss which has seismic velocity in the range of 4000-5100 m/s. It is overlain by thin sandy soil (as in c above) which is less than 5 m thick.

6.3 RECOMMENDATIONS

(1) Further measurements may be made between station Yo 400 m SW and Gida don Tanko to clearly define the extent of the anomaly there.

(2) Drill holes measurements should be carried out at several points on the pipe including such stations as X_2 45 m NW, anywhere between X_4 0 and X_4, 15 m NW, Yo 490 m SW and may be around Yo 380 m SW with a view to determine more accurately the structure and the intrinsic physical parameters of the geologic layers of the pipe. The holes may serve as reliable reference points for further work.

(3) It is possible that other kimberlite pipes may exist at the intersection of lineament and fracture zones and also at the junction between the major transcurrent fault and the displaced metasediment belt. A thorough mapping of the junction and the structural trend-lines using ground geological method may be carried out. This should be followed up with extensive regional and detailed magnetic and or gravity surveys of the intersection of the faults and linements to see if buried intrusions might exist. The anomalous areas should further be surveyed with electrical resistivity method which will delinate the anomalies in greater details.

(4) In order to determine the velocity and thickness of the top surface layer accurately, weathering spreads would need to be recorded over the country rock as well as on the kimberlite pipe. In such weathering spreads a geophone interval of 2-3 m may be used with shotpoints located at distances of about 3 m from the geophone nearest the shotpoint.

(5) Kimberlite pipes are known to be associated with considerable amount of water. On the basis of the present results the low apparent resistivities may be an indication that test dug wells located anywhere along the strike of the Masari/Kafur kimberlite pipe and also near station Yo 500 m SW may yield water. However the seismic results show that within the pipe the ground water is probably nearer the ground surface at near station Yo 380 m SW.

REFERENCES

1. Bateman, A. M., 1967, Economic Mineral Deposits, J. Wiley and Sons Inc. New York p. 837-839.

2. Battacharya, P. K. and Patra H. P., 1968, Direct Current Geoelectrical Sounding, Elsevier Publishing Company, Amsterdam.

3. Clifford, T. M., 1972, Location of Mineral Deposits, in: Understanding the Earth, ed. IG Gass, P. J. Smith, R. C. L. Wilson, MIT Press p. 319-322.

4. - 1968, Recent Researches of Kimberlite and Diamond Geology, Economic Geology, Vol. 63, No. 5, p.

6. Dobrin, M. B., 1976, Introduction to Geophysical Prospecting McGraw-Hill, New York.

7. Gerryts, E., 1967, Diamond Prospecting by Geophysical Methods - a Review of Current Practice, in: Mining and ground water Geophysis. Geological Survay of Canada.

8. Grant, F. S. and West, G. F., 1969, Interpretation Theory in Applied Geophysics. McGraw-Hill, New York.

9. Green, R., 1974, The Seismic Refraction Method - a Review. Geoexploration Vol. 12 p.259-284.

10. Hagedoorn, J. G., 1959, The Plus-Minus Methods of Interpreting Seismic Refraction Sections. Geophysical Prospecting, Vol. 7, p. 167-182.

11. Hawkins, L. V., 1961, The Reciprocal Method of Routine Shallow Seismic Refraction Investigations. Geophysics, Vol. 26, No. 6, p. 806-819.

12. - 1969, Seismic Refraction Surveys, for Civil Engineering, Geophysical Memorandum 2/69 Atlas Copco Abem, Sweden.

13. Hobson, G. D., 1967, Seismic Methods in Mining and Groundwater Exploration, in: Mining and Groundwater Geophysics/1967. Economic Geology Report No. 26, Geological Survey of Canada.

14. Keller, G., and Frischknecht, F., 1977, Electrical Methods in Geophysical Prospecting, Pergamon Press New York.

15. Kunetz, G., 1966, Principles of Direct Current Resistivity Prospecting, Geopublication Associates, Berlin-Nikolasee.

16. Lenox, H., and Carlson V., 1967, Geophysical Exploration for Buried Valleys. Geophysics Vol. 32, p. 231.

17. McCurry, P., 1970, The Geology of Degree sheet 21 (Zaria). M.Sc. Thesis, Ahmadu Bello University, Zaria.

18. Mooney, H. M., 1977, Handbook of Engineering Geophysics Bison Instruments Inc, Minnesota.

19. Parish, J. B., 1978, The Relationship of Geophysical and Remote Sensing Lineaments to Regional Structure and Kimberlite intrusions in the Appalachian. Plateau M.Sc. Thesis, Pennsylvania State University, U.S.A.

20. Peterson, N. R., Mac Fadyen, D. A., and Arif Turkeli, 1977; Geophysical Exploration for Kimberlites with Special Reference to Lesotho (Per Comm.)

21. Rijkswaterstaat, 1975, Standard Graphs for resistivity Prospecting. EAEG, The Netherlands.

22. Telford, W. M. Geldart, L. P., Sheriff, R. E., Keys, D. A., 1976, Applied Geophysics, Cambridge University Press. London.

23. Turner, D. C., 1975, A note on Supposed Kafur Kimberlite. Unpublished Report.

24. Wright, J. B., 1976, Volcanic Rocks in Nigeria, in: Geology of Nigeria ed. C. A. Kogbe, Elizabethan Publication Co. Ibadan p. 96-97.

25. Verhoijen, P. J. T. and Ajakaiye, D. E., 1979, Geophysical Exploration of a Suspected Kimberlite Pipe in the Metamorphic Schist Belt of Northern Nigeria. Geoexploration (in Press).

26. Vingoe, P., 1972, Electrical Resistivity Surveying, Geophysical Memorandum 5/72, Atlas Copco ABEM, Sweden.

27. Zijl, J. S. V., 1969, A deep Schlimberger Sounding to Investigate the Electrical Structure of the Crust and Upper Mantle in South Africa. Geophysics, Vol. 34, No. 3, p. 450-462.

28. Zhody, A. A. R., 1969, The use of Schlumberger and Equatorial Soundings in Groundwater Investigations near El Paso, Texas. Geophysics, Vol. 34, No. 5, p. 713-728.